Gondwana Research 83 (2020) 63–79

Contents lists available at ScienceDirect

Gondwana Research

journal homepage: www.elsevier.com/locate/gr

Formation and evolution of the Eastern Kunlun Range, northern Tibet: Evidence from detrital zircon U-Pb geochronology and Hf isotopes

Xing Jian [a,*], Amy Weislogel [b], Alex Pullen [c], Fei Shang [d]

[a] State Key Laboratory of Marine Environmental Science, College of Ocean and Earth Sciences, Xiamen University, Xiamen 361102, PR China
[b] Geology and Geography, West Virginia University, 98 Beechurst Ave, Morgantown, WV 26506, USA
[c] Department of Environmental Engineering and Earth Sciences, Clemson University, Clemson, SC 29634, USA
[d] Research Institute of Petroleum Exploration and Development (RIPED), PetroChina, Beijing 100083, PR China

ARTICLE INFO

Article history:
Received 9 October 2019
Received in revised form 8 January 2020
Accepted 18 January 2020
Available online 28 February 2020

Handling Editor: Z.M. Zhang

Keywords:
Tibetan Plateau
Eastern Kunlun
Qaidam basin
Precambrian
Detrital zircon U-Pb geochronology

ABSTRACT

The Eastern Kunlun Range, as a high-elevation and granitoid-rich tectonic element in northern Tibet, records Paleozoic–Mesozoic amalgamation process of the East Asia continent and Cenozoic uplift of the Tibetan Plateau. However, Precambrian evolution of the Eastern Kunlun remains poorly understood and relations between Eastern Kunlun and adjacent terranes (e.g., Qaidam and Qilian) during the Phanerozoic accretion process are still highly controversial. We use detrital zircon U-Pb geochronological and Hf isotopic data of Proterozoic and Paleozoic metasedimentary rocks from the Eastern Kunlun Range, to reconstruct its origin and subsequent evolutionary history. Detrital zircons of the Proterozoic rocks are dominated by early–middle Neoproterozoic ages (700–1000 Ma), with two age peaks at ca. 800 Ma and ca. 920 Ma and εHf(t) values ranging from −10 to 5. The youngest detrital zircon ages (648–788 Ma) demonstrate that these investigated Proterozoic strata, which were previously mapped as Paleoproterozoic to Mesoproterozoic, were most likely deposited in the middle–late Neoproterozoic. Abundant 0.9–1.0 Ga detrital zircon crystals are consistent with those crystalline rocks of similar ages across the Kunlun-Qaidam and Qilian terranes, which are generally interpreted as the product of Grenvillian orogenesis. These findings support the hypothesis that these terranes were probably within a single continental landmass (named as KQQ block) during the Neoproterozoic. The high similarity of detrital zircon ages, Hf isotopes and Neoproterozoic lithostratigraphy between western Yangtze and KQQ blocks, supports a temporary connection of the KQQ block to western Yangtze in Rodinia supercontinent. Detrital zircons of the analyzed Paleozoic rocks are characterized by 390–490 Ma age populations. These results, in combination with published granitoids data of the northern Tibet, favor a scenario in which the Kunlun-Qaidam and Qilian terranes underwent separated subduction and accretion processes during the late Cambrian–Devonian, but together formed an upper plate to northward subduction of the Paleo-Tethys during the Permian–Triassic.

1. Introduction

The Kunlun Range, located in the northern part of the Tibetan Plateau (Fig. 1A), is a ~2500 km-long, latitudinally-trending, high-elevation (>5000 m) and granitoid-rich zone in central China (Xu et al., 1999; Cowgill et al., 2003; Mo et al., 2007; Dong et al., 2018; Mu et al., 2018; Pei et al., 2018). The Kunlun Range has been divided into eastern and western parts (i.e., Eastern Kunlun and Western Kunlun Ranges) by Cenozoic left-lateral strike slip motion on the Altyn Tagh fault (Fig. 1). In addition to recording the Cenozoic upward and outward growth of the Tibetan Plateau (e.g., Yin and Harrison, 2000; Jolivet et al., 2001; Tapponnier et al., 2001; Wang et al., 2008; Clark et al., 2010), the geologic record in the Kunlun Range also preserves multiple cycles of ocean subduction, closure and continent amalgamation prior to Cenozoic (Mattern and Schneider, 2000; Xiao et al., 2002; Mo et al., 2007; Gehrels et al., 2011; Dong et al., 2018; Song et al., 2018; Wu et al., 2019a,b,c).

The Phanerozoic tectono-magmatic history and accretionary process of the Eastern Kunlun have been well documented (e.g., Cowgill et al., 2003; Liu et al., 2005; Zhu et al., 2006; Dai et al., 2013; Li et al., 2013, 2015a,b; Xiong et al., 2014, 2015; Hu et al., 2016; Zhou et al., 2016; Shao et al., 2017; Zheng et al., 2018; Wu et al., 2019a,b,c). It is widely recognized that the Eastern Kunlun was intruded by arc magmas in response to successive subduction of the Proto-Tethys and Paleo-Tethys oceans and felsic magmas in response to continental collisions during the Paleozoic to Triassic (e.g., Gehrels et al., 2011; Li et al., 2013; Zhang et al., 2017b; Dong et al., 2018; Mu et al., 2018; Song et al., 2018). However, relationships between the Kunlun-Qaidam and Qilian terranes in the Paleozoic–Mesozoic multiple Wilson cycles remain

* Corresponding author.
E-mail address: xjian@xmu.edu.cn (X. Jian).

https://doi.org/10.1016/j.gr.2020.01.015

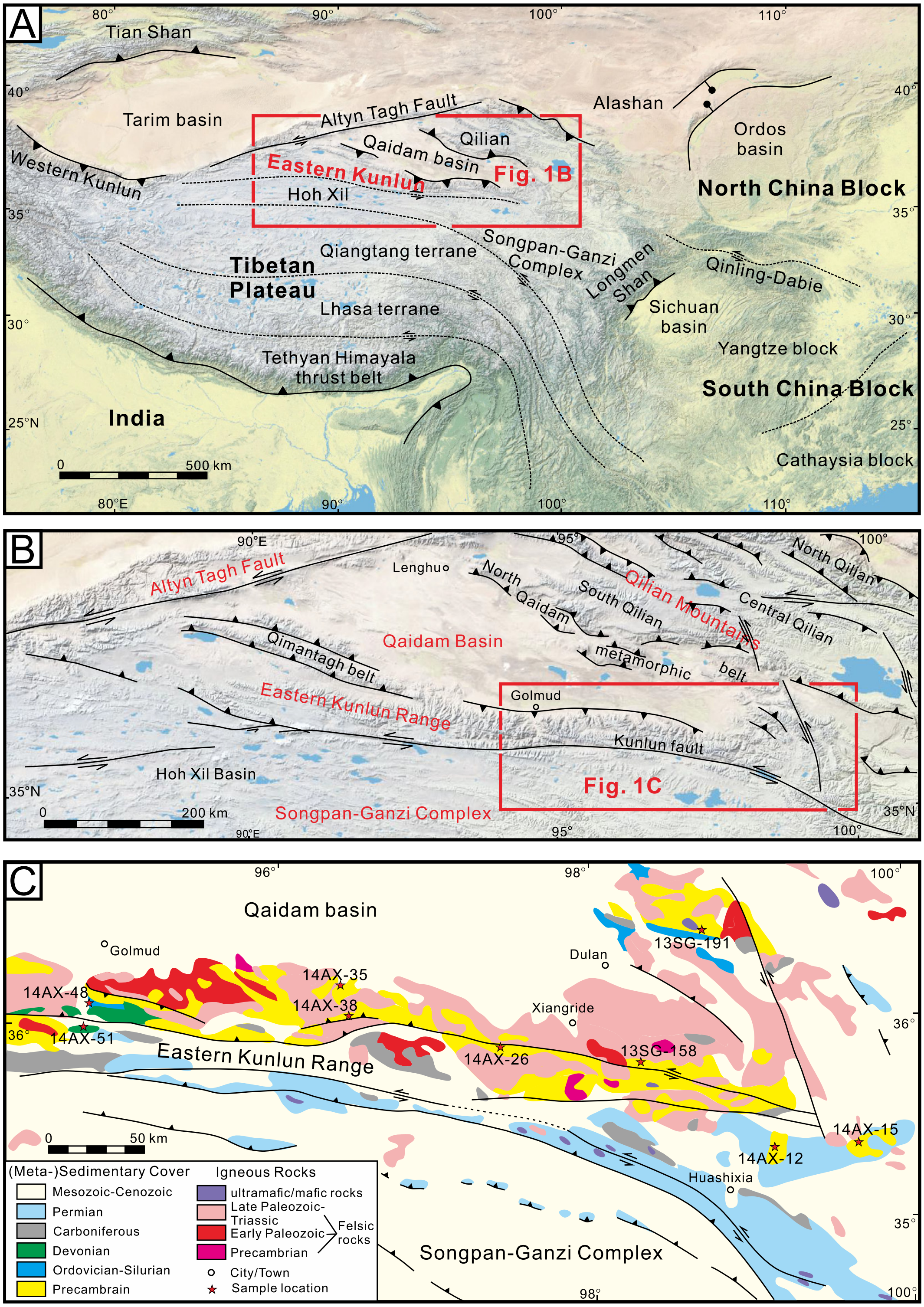

Fig. 1. (A) A map showing major tectonic elements of the Tibetan Plateau and surrounding regions. (B) Location of the Eastern Kunlun Range, modified from Jian et al. (2018). (C) Geological map of the eastern part of the Eastern Kunlun Range and sample locations.

widely debated. Two of the more widely accepted tectonic models for the Paleozoic–Mesozoic include: 1) an archipelago model posits that the terranes were separated from each other by ocean basins during the early Paleozoic and amalgamated together during the mid- to late Paleozoic (e.g., Hsu et al., 1995; Yin and Harrison, 2000; Yin et al., 2007; Gehrels et al., 2003a), or 2) a continuous continent by the early Paleozoic in which the Qaidam-Qilian terrane was sandwiched between the North Qilian arc to the north and the Kunlun arc to the south (e.g., Song et al., 2013, 2014; Cheng et al., 2017). More work is necessary to differentiate between these models or propose new ones describing the Phanerozoic accretionary history of northern Tibet.

By contrast, Precambrian evolution of the Eastern Kunlun Range is more poorly understood, but it is important for better understanding of formation and growth of the Tibetan Plateau and for defining the architecture of supercontinents and the Tibetan crust. Previous studies proposed that the Eastern Kunlun underwent three episodes of tectono-magmatic events during the Precambrian, occurring at 2400–2500 Ma, 1800–1900 Ma and ca. 1000 Ma (BGMRQP, 1991; Wang et al., 2007). The Precambrian sedimentary strata in the Eastern Kunlun Range have been highly metamorphosed or deformed. According to the dating of interbedded volcanic rocks and igneous intrusions (BGMRQP, 1991; Pan et al., 2004; Chen et al., 2006, 2011; Wang et al., 2007; Zhang et al., 2012; Dong et al., 2018 and references therein) and fossil identifications for some Binggou Group sedimentary strata (e.g., BGMRQP, 1991; Luan et al., 2011), most of these Precambrian strata were previously thought to be deposited prior to Neoproterozoic. However, recently, a growing number of investigations indicated maximum depositional ages of the Neoproterozoic for some Precambrian outcrops in the Eastern Kunlun Range (Liu et al., 2016; Zhang et al., 2018a; Wu et al., 2019b).

The widespread early Neoproterozoic (900–1000 Ma) igneous rocks in northern Tibet, are generally interpreted to have resulted from Grenvillian orogenesis during collisional-related tectonic events; and the general consensus is that these terranes were involved in the amalgamation of the Rodinia supercontinent during the Neoproterozoic (e.g., Lu, 2002; Gehrels et al., 2003b; Chen et al., 2007a; Song et al., 2012; Yu et al., 2013, 2019b; He et al., 2016a, 2016b, 2018; Cheng et al., 2017; He et al., 2018). It has been proposed that the Kunlun-Qaidam and Qilian terranes were connected with the Yangtze block within the Rodinia supercontinent, based on the similar ages and petrogenesis of the early Neoproterozoic igneous rocks from these two regions (e.g., Song et al., 2012; Tung et al., 2012; Yu et al., 2013). However, the Yangtze block is characterized by widespread middle Neoproterozoic (ca. 720–900 Ma) igneous rocks and middle–late Neoproterozoic sedimentary covers (Liu et al., 2008; Wang et al., 2010, 2012a, 2013), rock of this age and characteristics have not been widely observed in the Eastern Kunlun (BGMRQP, 1991; Wang et al., 2007; Dong et al., 2018). Because of this incongruity, we tested the tectonic affinity of the Proterozoic rocks that compose the continental core of the Eastern Kunlun to better understand its role in the formation and breakup of the Rodinia supercontinent.

Here, we present new detrital zircon U-Pb geochronology and Hf isotope results for Proterozoic and Paleozoic sedimentary rocks from the eastern part of the Eastern Kunlun Range and combine published data to unravel the formation and pre-Mesozoic evolution of the range.

2. Geological setting

2.1. Background of the northern Tibet

The Eastern Kunlun Range is located to the west of the Qinling-Dabie orogenic belt, neighboring the Qaidam basin and Qilian mountains on the north and the Songpan-Ganzi Complex on the south (Fig. 1A). The Western Kunlun Range, exhibiting largely the same pre-middle Cenozoic geology as the Eastern Kunlun, is considered to represent the western continuation of the same subduction-accretionary belt (Yin and Harrison, 2000; Xiao et al., 2002, 2005; Cowgill et al., 2003). The left-lateral strike slip along the Altyn Tagh Fault has resulted in a cumulative ca. 375 km offset between these two ranges (Gehrels et al., 2003b; Yue et al., 2004; Cheng et al., 2015; Wu et al., 2019d).

The Qinling-Dabie orogenic belt formed by the convergence and continent-continent collision between the North China and South China blocks by the Triassic (Meng and Zhang, 2000; Hacker et al., 2004; Dong et al., 2011; Li et al., 2014a,b; Dong and Santosh, 2016). The Songpan-Ganzi Complex is characterized by thick and widespread deep water oceanic calciclastic and siliciclastic gravity flow deposits identified as the largest Triassic accumulation of sediments on earth. These flysch deposits were extensively intruded by Late Triassic–Early Jurassic igneous rocks, have been highly deformed and preserve rich records of late-stage evolution and closure of the Eastern Paleo-Tethys ocean (Weislogel et al., 2006, 2010; Pullen et al., 2008; Ding et al., 2013; Zhang et al., 2014; Jian et al., 2019a). The Qilian mountains, which are expressed as a ~300 km wide fold-thrust belt (Fig. 1B; Yin and Harrison, 2000; An et al., 2018; Zuza et al., 2018; Cheng et al., 2019a,b), form the northern most high topography of the Tibetan Plateau (Fig. 1A) and from north to south consist of the North Qilian early Paleozoic complex, the Central Qilian Proterozoic basement and the South Qilian-North Qaidam ultra-high pressure metamorphic belt (Fig. 1B). The Qilian mountains are mainly composed of different types of metamorphic rocks, volcanic rocks, marine sedimentary strata as well as ophiolite suites (Gehrels et al., 2003a,b; Tung et al., 2007a,b; Xiao et al., 2009; Song et al., 2013, 2014) and have experienced multiple episodes of tectonic deformation, including Neoproterozoic continental breakup, early Paleozoic subduction and continental collision, Mesozoic extension and Cenozoic intracontinental orogenesis (Zuza et al., 2018 and reference therein; Yu et al., 2019a,b,c). The Qaidam basin is a non-marine Mesozoic–Cenozoic petroliferous basin and stores sediments derived from the surrounding Eastern Kunlun, Qilian and Altun mountains (Zhuang et al., 2011; Wu et al., 2011; Jian et al., 2013a,b, 2014, 2018, 2019b; Cheng et al., 2014, 2015, 2019b; Wei et al., 2016; Bao et al., 2017; Yu et al., 2017; Lu et al., 2018; Zhang et al., 2018b). The Qaidam basin was involved into three tectono-magmatic episodes (i.e., early Neoproterozoic, early Paleozoic and late Paleozoic–earliest Mesozoic) and is regarded as a tectono-magmatic rejuvenated terrane, rather than a rigid and mechanically-strong craton (Cheng et al., 2017). Therefore, the Qaidam and Eastern Kunlun together are generally regarded as a single terrane (so-called Kunlun-Qaidam terrane) having similar pre-Mesozoic history (e.g., Yin and Harrison, 2000; Dai et al., 2013; Wu et al., 2016, 2019a, 2019b, 2019c; Cheng et al., 2017; Zuza et al., 2018).

2.2. Precambrian–Paleozoic stratigraphy of the Eastern Kunlun

The geology of the Kunlun-Qaidam terrane is best exposed in the Eastern Kunlun Range along the south margin of the terrane. The Precambrian sedimentary strata in north regions of the Eastern Kunlun Range were named as Jinshuikou Group (containing Baishahe Group and Xiaomiao Formation) and Binggou Group (containing Langyashan and Qiujidonggou Formations); and those in the south regions of the Eastern Kunlun Range were named as Kuhai Group and Wanbaogou Group (Fig. 2). The Precambrian sedimentary strata are unconformably overlain by early Paleozoic marine sedimentary successions and mainly consist of genesis, schist, quartzite, amphibolite, slate and marble rocks (Fig. 2; Pan et al., 2004). These strata were intruded by foliated granitoids and have been metamorphosed. Most of these Precambrian strata were thought to form in shallow marine depositional settings of continental margins, as they are characterized by mixed carbonate-siliciclastic and volcanic successions (Wang et al., 2007; Chen et al., 2011; Luan et al., 2011). Previous studies reported 1.93 Ga interbedded meta-basite in the Baishahe Group, 1.85 Ga and 820–940 Ma meta-granite intrusions in the Xiaomiao Formation and Kuhai Group and 1300–1500 Ma volcanic rocks within the Wanbaogou Group strata, suggesting that these sedimentary strata were probably deposited in the Paleoproterozoic–Mesoproterozoic (A et al., 2003; Pan et al., 2004; Wang et al., 2007 and references therein; Wei et al., 2007; Zhang et al., 2012; Wu et al., 2016). The discovery and identification results of micro-plant fossils and stromatolites reveal that the Langyashan and Qiujidonggou Formations in the Binggou Group were likely deposited in the Mesoproterozoic and early Neoproterozoic (BGMRQP, 1991; Luan et al., 2011), respectively. However, several detrital zircon age-based studies found that some metasedimentary rocks, mapped as Kuhai, Binggou (including the Langyashan Formation) and Wanbaogou Groups have maximum depositional ages of the Neoproterozoic (Liu et al., 2016; Zhang et al., 2018a; Wu et al., 2019b). The Wanbaogou Group was also reported to be deposited in the Neoproterozoic, based on the new age data (ca. 762 Ma) of the basalt layers (Xu et al., 2016).

The Ordovician–Silurian Nachitai Group is mainly composed of volcanic rocks, volcaniclastic rocks and shallow- and deep-marine (meta)

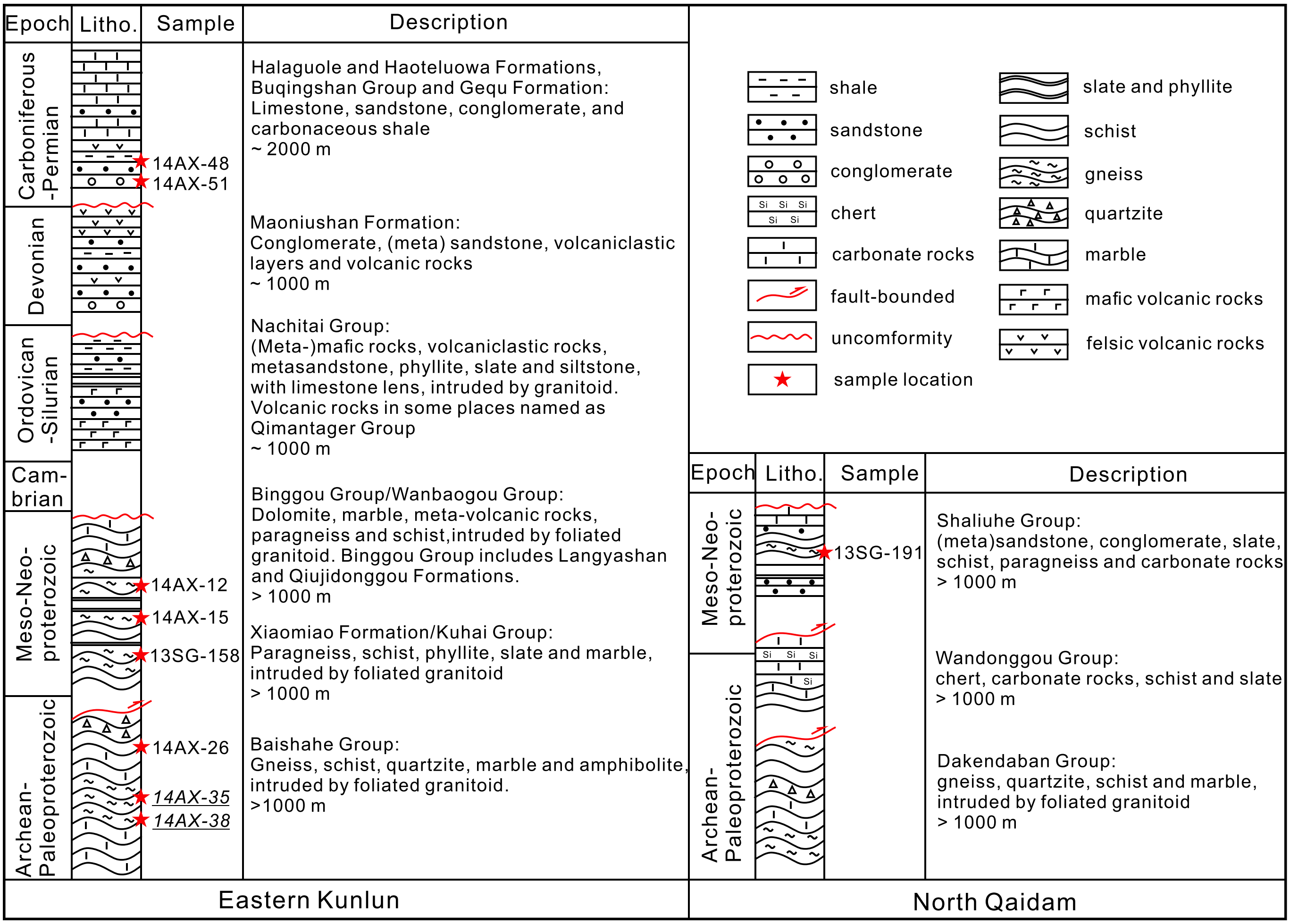

Fig. 2. Simplified regional stratigraphic sections and descriptions of the Eastern Kunlun Range and the North Qaidam metamorphic belt, compiled from BGMRQP (1991) and Pan et al. (2004). Stratigraphic attributions of the analyzed samples are based on 1:200000 geological maps. Note that the samples 14AX-35 and 14AX-38, which were previously mapped as Baishahe Group, were most likely deposited in the Paleozoic based on the new detrital zircon age data in this study.

siliciclastic rocks and limestones, probably representing an arc sequence (Pan et al., 2004). The Devonian molasse Maoniushan Formation (also named as Heishangou and Haerzha Formations) overlies those Precambrian and Ordovician–Silurian strata with an angular unconformity (Wu et al., 2019b) and consists of conglomerates, sandstones, volcanic rocks and volcaniclastic layers. The molasse formation was thought to form in terrigenous or shallow-water depositional environments (Chen et al., 2007b). A couple of rhyolite interlayers therein indicate 400–420 Ma U-Pb ages (Lu et al., 2010; Peng et al., 2016; Qi et al., 2018), suggesting the possible depositional ages of Early Devonian for the Maoniushan Formation strata. The overlying Carboniferous–Permian sedimentary succession (including Halaguole and Haoteluowa Formations, Buqingshan Group and Gequ Formation) is characterized by shallow marine mixed carbonate-siliciclastic sequences and deep-water flysch sedimentary successions with volcaniclastic layers (Fig. 2). Each sequence within the Carboniferous–Permian strata is presented by lower siliciclastic rock-dominated conglomerates, arkosic and quartz sandstones and upper carbonate rock-dominated limestones, carbonaceous shales and calcareous siltstones (Wu et al., 2019b). Furthermore, mafic-ultramafic intrusive rocks and ophiolitic fragments occur as tectonic lenses within a high-grade metamorphic complex in the north of the Kunlun fault. The formation of these rocks remains an open question. It has been interpreted as indicating either an early Paleozoic suture (e.g., Yang et al., 1996, 1999; Meng et al., 2013, 2015) or a back-arc basin (e.g., Mo et al., 2007; Li et al., 2013; Dong et al., 2018) in the Eastern Kunlun regions. The details of geological settings, lithology and ages of those exposed rocks are described by BGMRQP (1991) and Pan et al. (2004).

3. Samples and methods

Depositional ages and sediment provenance of these Proterozoic and Paleozoic strata remain poorly understood. Eight metasedimentary rocks from the Eastern Kunlun Range and one metasedimentary rock (13SG-191) from the North Qaidam metamorphic belt (Fig. 1C) were collected for detrital zircon U-Pb geochronology and Hf isotope analysis. The detailed descriptions of the analyzed samples are shown in Table 1. Representative outcrop features and photomicrographs of these samples are shown in Fig. 3. The investigated Proterozoic and Paleozoic outcrops have been metamorphosed to variable grades, including slightly metamorphosed, greenschist facies and amphibolite facies (Fig. 3). Petrography observations demonstrate that staurolite and garnet minerals are present in samples 14AX-12 and 14AX-38, indicating that these related sedimentary strata have experienced amphibolite facies metamorphism. The slightly metamorphosed sandstone samples (e.g., 13SG-158, 14AX-26 and 14AX-48) remain the texture of typical clastic rocks (Fig. 3D–E).

Zircon grains were separated and then mounted in epoxy, polished, imaged with a SEM to define the internal structure of the grains, and analyzed at the University of Arizona LaserChron Center using techniques described by Gehrels et al. (2006) and Gehrels and Pecha (2014). Sri Lanka and R33 zircon fragments were employed as zircon standard

Table 1
Description of the analyzed metasedimentary rock samples and major detrital zircon U-Pb age peaks.

Sample	Tectonic unit	Latitude	Longitude	Lithology	Stratigraphic unit[a]	MDA (Ma)[b]	Major detrital zircon peak ages[c]
13SG-191	NQ	36.4619	98.6252	Mica schist (greenschist facies)	Shaliuhe Group	766 ± 20 (2)	928 Ma (33)
13SG-158	EK	35.8057	98.2826	Metasandstone (slightly metamorphosed)	Xiaomiao Formation	732 ± 36 (4)	928 Ma (44)
14AX-12	EK	35.3372	99.1825	Garnet-mica schist (low-amphibolite facies)	Kuhai Group	648 ± 1 (3)	806 Ma (25)
14AX-15	EK	35.2492	99.6156	Mica-quartz schist (greenschist facies)	Kuhai Group	788 ± 10 (9)	805 Ma (18)
14AX-26	EK	35.8410	97.4086	Metasandstone (slightly metamorphosed)	Baishahe Group	660 ± 21 (3)	940 Ma (104)
14AX-35	EK	36.2161	96.4021	Biotite schist (greenschist facies)	Baishahe Group?	434 ± 6 (2)	442 Ma (3)
14AX-38	EK	36.0344	96.4522	Biotite-plagioclase paragneiss (amphibolite facies)	Baishahe Group?	381 ± 3 (2)	434 Ma (21)
14AX-48	EK	35.9728	94.8167	Metagreywacke (slightly metamorphosed)	Lower Permian	469 ± 4 (51)	473 Ma (75); 978 Ma (28)
14AX-51	EK	35.8407	94.7377	Metaconglomerate (greenschist facies)	Lower Permian	403 ± 6 (2)	430 Ma (70)

NQ: North Qaidam metamorphic belt; EK: Eastern Kunlun.
[a] The stratigraphic units for the samples are based on geological maps (1:200,000) (BGMRQP, 1991), which deserve re-evaluation. For the details, see the Section 5.1.
[b] MDA: maximum depositional age. Here we use the youngest grain cluster at 2σ uncertainty for each sample. Zircon grains with U/Th ratio >10 were excluded for the MDA calculation. The numbers in the brackets indicate the amounts of the zircon ages for the MDA calculation.
[c] The peak ages are obtained using AGE PICK program of Arizona Laserchron Center (http://www.geo.arizona.edu/alc/Analysis%20Tools.htm). The peaks ages shown here match with KDE plots (Fig. 4). The number in the bracket is the amount of detrital zircon grains supporting the corresponding peak age.

reference materials. Hf isotope analyses were conducted on top of the pits left after U-Pb analysis, to ensure that Hf isotope data were collected from the same domain as the U-Pb ages. Analyses were conducted by LA-MC-ICP-MS using a Photon Machines 193 nm excimer laser connected to the Nu Plasma HR ICP-M. The analyzed zircons have highly concordant $^{206}Pb/^{238}U$ and $^{207}Pb/^{235}U$ ages (Fig. A1 in the Supplemental material). The correction for initial-Pb on $^{206}Pb/^{238}U$ and $^{206}Pb/^{207}Pb$ was based on a ^{204}Hg-corrected measured ^{204}Pb. Ages <900 Ma are based on initial-Pb corrected $^{206}Pb/^{238}U$ ratios, whereas ages >900 Ma are based on initial-Pb corrected $^{206}Pb/^{207}Pb$ ratios. A total of 117 detrital zircon crystals (including dominant Neoproterozoic zircons and subordinate early Paleozoic and pre-Neoproterozoic zircons) were selected from 4 samples (13SG-158, 14AX-12, 14AX-26 and 14AX-38) for Hf isotope analyses. εHf (0), εHf (t) (t represents the zircon crystallization time) and Hf crustal model ages (T_{DM2}) for the analyzed zircons were calculated following Gehrels and Pecha (2014) and Wu et al., 2007b.

Full detrital zircon U-Pb age and Hf isotope data are shown in Tables S1 and S2 (in the Supplemental material), respectively.

4. Results

4.1. Detrital zircon U-Pb ages

We report a total of 867 detrital zircon U-Pb ages from the 9 samples and 850 U-Pb ages therein are concordant ages (the discordance between $^{206}Pb/^{238}U$ and $^{207}Pb/^{235}U$ ages <15% and reverse discordance <10%, see Table S1 and Fig. A1 in the Supplemental material). The analyzed detrital zircon crystals range from 65 to 200 μm. Most zircon crystals in the Proterozoic samples are sub-rounded to rounded, whereas the zircon crystals in the Paleozoic samples are dominantly sub-angular to sub-rounded in shape (Fig. A2 in the Supplemental material). Most analyzed zircons are characterized by oscillatory zoning textures

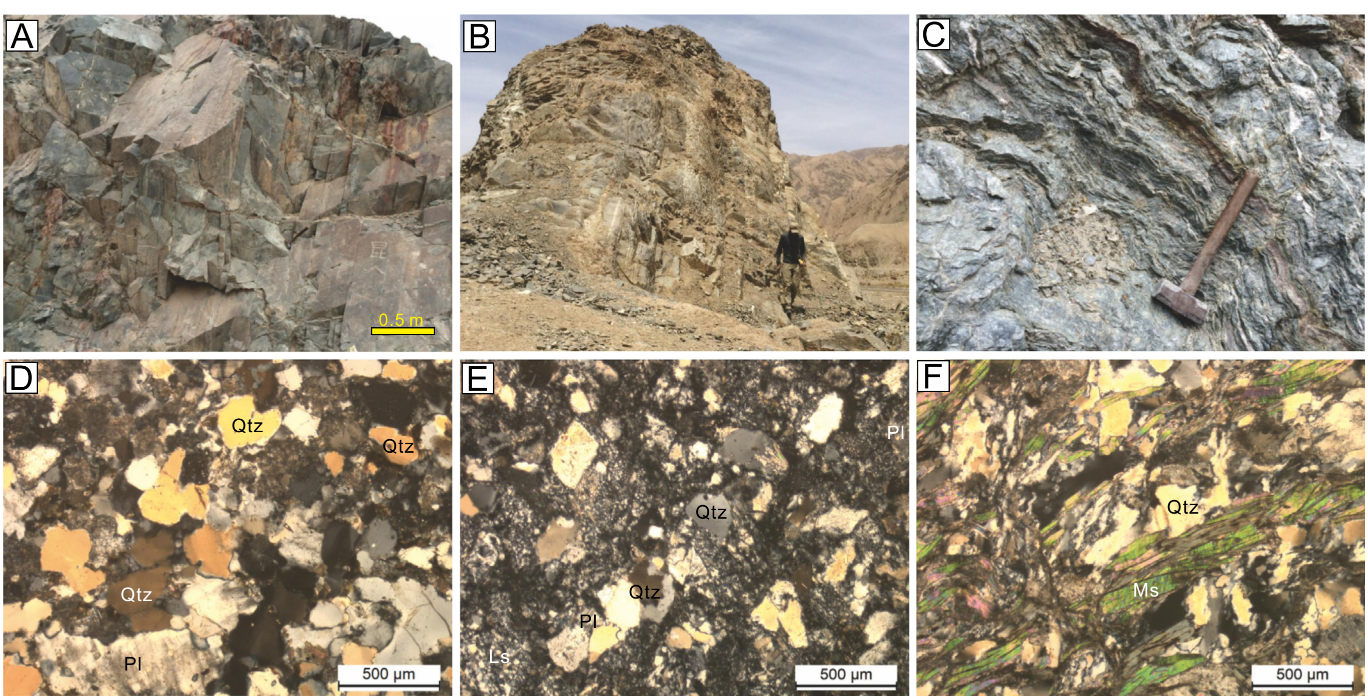

Fig. 3. Representative outcrop features and photomicrographs of the analyzed (meta-)sedimentary rock samples. (A) Lower Permian deep-water flysch sedimentary succession (14AX-48); (B) mylonitic paragneiss (14AX-38), mapped as Proterozoic Baishahe Group; (C) Proterozoic Kuhai Group mica-quartz schist (14AX-15); previous geological survey inferred that these two metasedimentary strata were deposited in shallow-water marine depositional settings of continental margins (BGMRQP, 1991; Wang et al., 2007). (D) Slightly metamorphosed, highly mature sandstone (14AX-26), dominated by quartz; (E) poorly sorted flysch metagraywacke (14AX-48), with abundant feldspar and lithic fragments; (F) mica schist (13SG-191), with the metamorphic grade of greenschist facies. The details of these samples are shown in Table 1. Qtz: quartz; Pl: plagioclase; Ls: sedimentary lithic fragment; Ms: muscovite.

(Fig. A2) and have quite low U/Th ratios (U/Th < 10) (Table S1), except some crystals from samples 14AX-26, 14AX-35 and 14AX-38 (Fig. A3 in the Supplemental material).

One hundred and seventy-six analyzed zircons of sample 14AX-26 are dominated by Neoproterozoic ages, with a peak at 940 Ma. Sample 13SG-158 has similar zircon age populations (a total of 75 usable grains with concordant ages) with sample 14AX-26 and shows an age peak at 928 Ma (Table 1). The detrital zircons of sample 13SG-191 from the North Qaidam belt primarily show Neoproterozoic ages (746–985 Ma), with one peak age at ca. 928 Ma and several Mesoproterozoic (1015–1600 Ma) ages (Fig. 4). Eighty detrital zircons of sample 14AX-12 are dominated by Neoproterozoic ages, with a peak at 806 Ma. Sample 14AX-15 (37 zircon grains) has similar zircon age distributions with the sample 14AX-12 and indicates a Neoproterozoic age peak at 805 Ma (Table 1).

The obtained 181 detrital zircon U-Pb ages of sample 14AX-48 cluster into two main probability peaks at 473 Ma and 978 Ma (Table 1; Fig. 4). Detrital zircons of samples 14AX-35 and 14AX-38 are featured by Middle Ordovician–Early Devonian (400–470 Ma) ages with the prominent probability peaks at 442 Ma and 434 Ma, respectively (Table 1). The 99 analyzed detrital zircons from sample 14AX-51 are overwhelmingly Middle Ordovician–Early Devonian (400–470 Ma) in ages (Fig. 4) with the prominent probability peak at 430 Ma (Table 1).

4.2. Detrital zircon Hf isotopes

The Hf isotopic results are illustrated in Fig. 5. Zircons that yielded crystallization ages in the range of 844–951 Ma ($n = 17$) in sample 13SG-158 yielded εHf(t) values in the range of −6.2–11.6 with a mean of −0.1 and standard deviation of 3.6. Zircon crystals in sample 14AX-26 in the range of 711–961 Ma ($n = 32$) yielded εHf(t) values in the range of −4.1–6.3 with a mean of 0.3 and standard deviation of 2.5. These zircons generally yielded Meso-Paleoproterozoic Hf crustal model (T_{DM2}) ages (1400–2000 Ma). However, the Neoproterozoic age detrital zircons (718–897 Ma) of sample 14AX-12 have much lower εHf(t) values (in the range of −17.8–8.3 with a mean of −8.3) and much older T_{DM2} ages (2000–2900 Ma) (Fig. 4). Neoproterozoic zircons in the sample 14AX-38 have similar Hf isotopic compositions to similar age zircons in samples 13SG-158 and 14AX-26 (Fig. 4). Furthermore, the Paleozoic detrital zircons in sample 14AX-38 primarily have negative εHf(t) values (mean of −3.2) and have similar Hf crustal

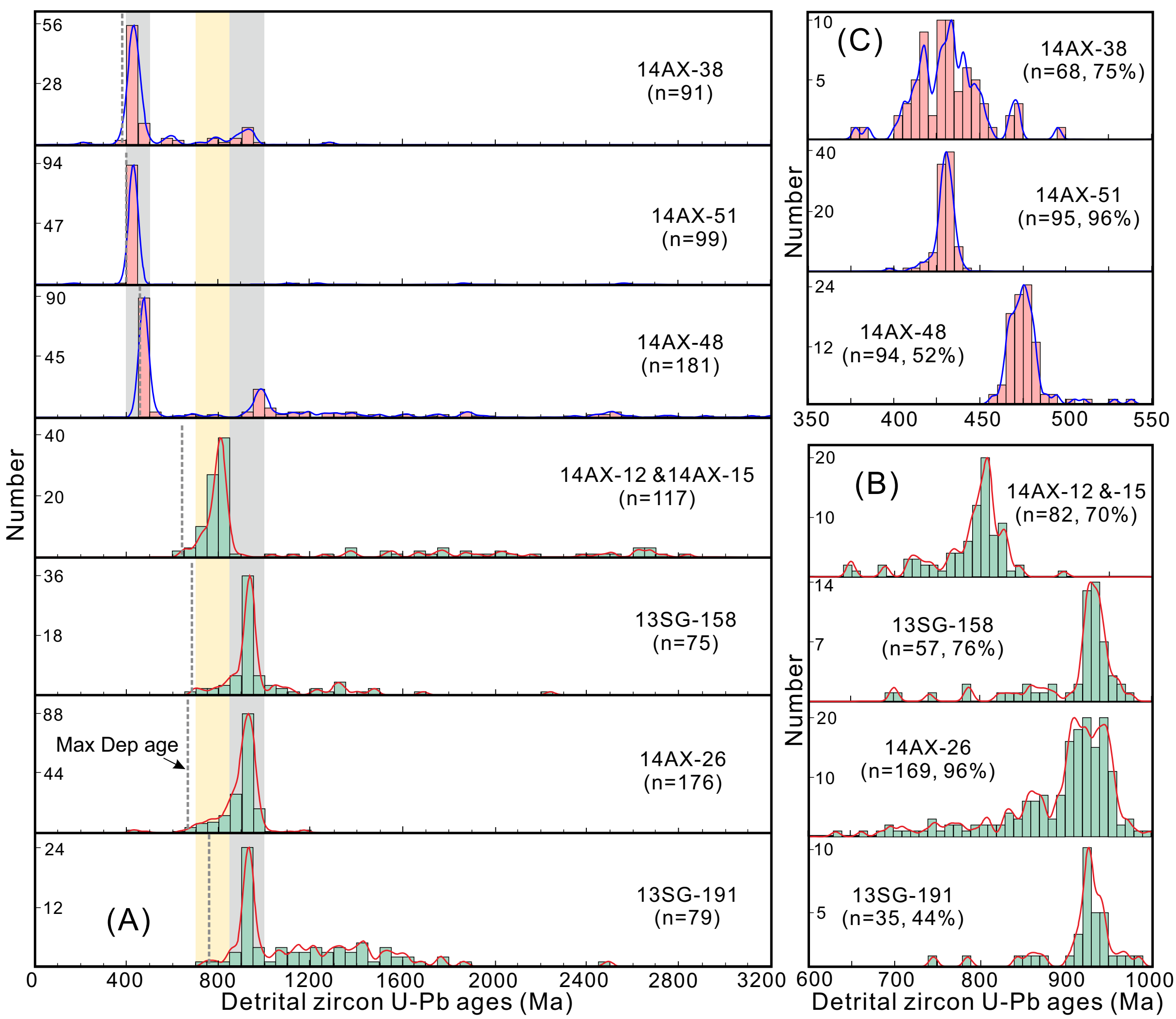

Fig. 4. Detrital zircon U-Pb age distribution of the (meta-)sedimentary rock samples. The dash lines show the maximum depositional ages (Max Dep age) for the samples. Note that all the analyzed samples show relatively concentrated detrital zircon U-Pb age peaks. Samples 13SG-158, 13SG-191, 14AX-12, 14AX-15 and 14AX-26 have dominant Neoproterozoic zircons, while samples 14AX-38, 14AX-48 and 14AX-51 have dominant Paleozoic zircons. All-age Kernel Density Estimation (KDE) plots (A), major Neoproterozoic age plots (B) and Paleozoic age plots (C) are drawn using bandwidth = 20, 5 and 2 in the DensityPlotter program (Vermeesch, 2012), respectively. Since only 29 and 37 zircon ages were obtained for the samples 14AX-35 and 14AX-15, respectively, the corresponding age plots are shown in Fig. A4 in the Supplement material for reference. As the samples 14AX-12 and 14AX-15 were collected from the same stratigraphic unit, closely with each other (Figs. 1–2) and have similar detrital zircon age populations, detrital zircon ages of these two samples were plotted together in this figure.

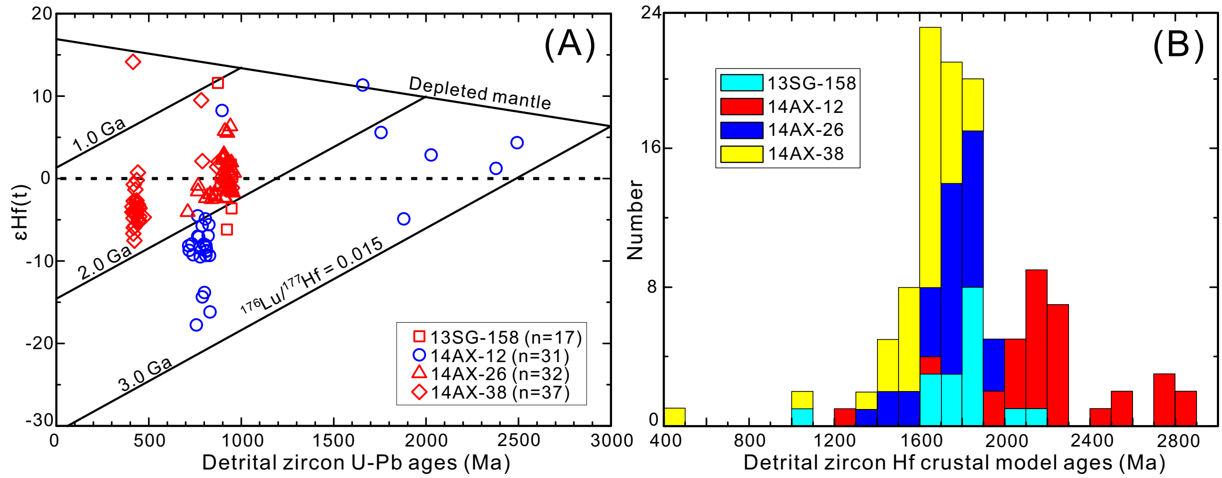

Fig. 5. Hf isotopic data of the selected detrital zircon samples. Note that the detrital zircons of middle Neoproterozoic ages (ca. 750–850 Ma) in sample 14AX-12 have more negative ε(Hf) values and older Hf crustal model ages than those early Neoproterozoic (ca. 900–1000 Ma) zircons in samples 13SG-158, 14AX-26 and 14AX-38. These analyzed Neoproterozoic detrital zircons have similar Hf isotopic compositions with igneous zircons of the Neoproterozoic collisional-related granitoids from the Eastern Kunlun Range (He et al., 2016b, 2018 and references therein).

model ages with those Neoproterozoic zircons of samples 13SG-158 and 14AX-26 which are in the range of 1400–2000 Ma (Fig. 4).

5. Discussion

5.1. Maximum depositional ages of the Proterozoic sedimentary strata

Detrital zircon U-Pb geochronology is a valuable approach to constrain the maximum depositional age (MDA) of sedimentary stratigraphic units by using the youngest U-Pb ages of igneous zircon grains in populations of detrital zircons (Dickinson and Gehrels, 2009; Spencer et al., 2016; Coutts et al., 2019). This is especially beneficial for Precambrian strata lacking biostratigraphic age control and for metasedimentary rocks like the Paleozoic strata described here lacking preserved fossils (e.g., Stewart et al., 2001; Barbeau et al., 2005; Jones et al., 2009). MDA calculation methods vary considerably and the most successful way to increase the accuracy of a calculated MDA is by acquiring a large number (n > ~300) of low-uncertainty measurements (Coutts et al., 2019). Here we use the youngest grain cluster at 2σ uncertainty (Coutts et al., 2019) to roughly constrain the MDA for the analyzed samples (Table 1).

The Baishahe and Kuhai Groups and the Xiaomiao Formation in the Eastern Kunlun Range were previously thought to be Paleoproterozoic to Mesoproterozoic (BGMRQP, 1991; A et al., 2003; Pan et al., 2004; Wang et al., 2007; Wei et al., 2007; Chen et al., 2011; He et al., 2016a; Dong et al., 2018). However, four analyzed samples (i.e., 13SG-158, 14AX-12, 14AX-15 and 14AX-26) from these three stratigraphic units yield youngest zircon U-Pb ages from 648 ± 1 Ma to 788 ± 10 Ma (Table 1; Fig. 4). The lack of mineral assemblages associated with high-grade metamorphism, oscillatory zoning textures and low U/Th ratios in the youngest zircon crystals (Figs. A2–A3) indicate that these youngest zircons were of igneous origin. This means that these investigated Proterozoic strata were most likely deposited in the middle–late Neoproterozoic. Similarly, several other Proterozoic sedimentary outcrops in the Eastern Kunlun Range, mapped as Jinshuikou Group, Kuhai Group or Langyashan Formation, have middle Neoproterozoic (750–800 Ma) MDAs (Liu et al., 2016; Zhang et al., 2018a). The stratigraphic age of the Wanbaogou Group, which was previously controversial (i.e., Mesoproterozoic or Neoproterozoic), can be confirmed as the Neoproterozoic by recent studies (Xu et al., 2016; Wu et al., 2019b). Note that samples 14AX-35 and 14AX-38 were collected from sedimentary strata mapped as Paleoproterozoic Baishahe Group, however, we infer that the stratigraphic ages of these two samples might be late Paleozoic because of the Silurian–Devonian MDAs (Table 1). Collectively, we suggest that the Proterozoic metasedimentary strata in the Eastern Kunlun Range deserve more attention and re-evaluation.

Likewise, sample 13SG-191 has a MDA at 766 ± 20 Ma (Table 1), supporting the premise that the Shaliuhe Group in the North Qaidam metamorphic belt was deposited during the middle–Late Neoproterozoic (BGMRQP, 1991; Pan et al., 2004). Furthermore, Neoproterozoic sedimentary strata have been recognized in several locations of the Qilian orogen based on youngest zircon age constrains or dating of igneous intrusions in the investigated strata (BGMRQP, 1991; Smith, 2006; Tung et al., 2007a,b; Yan et al., 2015). All these findings suggest that the middle–late Neoproterozoic sedimentary strata in the Eastern Kunlun, Qaidam and Qilian regions are more widely spread than previously known.

5.2. Provenance of the Proterozoic and Paleozoic sedimentary strata in the Eastern Kunlun Range

The detrital zircon U-Pb age data in this study (Fig. 4) indicate that detritus in the analyzed Baishahe Group and Xiaomiao Formation strata (i.e., samples14AX-26 and 13SG-158) was mainly derived from a source with widespread early Neoproterozoic (900–980 Ma) magmatism, whereas the analyzed Kuhai Group deposits (i.e., samples 14AX-12 and 14AX-15) were primarily sourced from regions where middle Neoproterozoic (750–850 Ma) magmatism prevailed. A compilation of published zircon U-Pb ages of granitoids in north Tibet (Fig. 6; Table S3) demonstrates widely distributed early Neoproterozoic (905–955 Ma) subduction- and collision-related granitoids in the Kunlun-Qaidam and Qilian terranes (Gehrels et al., 2003b; Tung et al., 2013; Huang et al., 2015; Cheng et al., 2017; He et al., 2018), which potentially provided sediments to the analyzed Baishahe Group and Xiaomiao Formation strata in the Eastern Kunlun Range. Middle Neoproterozoic granitoids have not been found in the Kunlun-Qaidam terrane, according to the investigations so far, but were discovered in the Qilian regions (Fig. 6; Tung et al., 2013). These middle Neoproterozoic igneous units (755–826 Ma) were possibly the sources for the analyzed Kuhai Group sedimentary strata in the Eastern Kunlun Range. Furthermore, the similarity of Hf isotopes between the analyzed Neoproterozoic zircon crystals (Hf(t) values ranging −17.8–11.6) and zircons in the Qilian granitoids (Hf(t) values ranging −15–10, Huang et al., 2015) also supports the provenance interpretation. Given that a great number of the analyzed detrital zircon crystals are rounded in shape (Fig. A2) and Neoproterozoic strata in the Eastern Kunlun Range

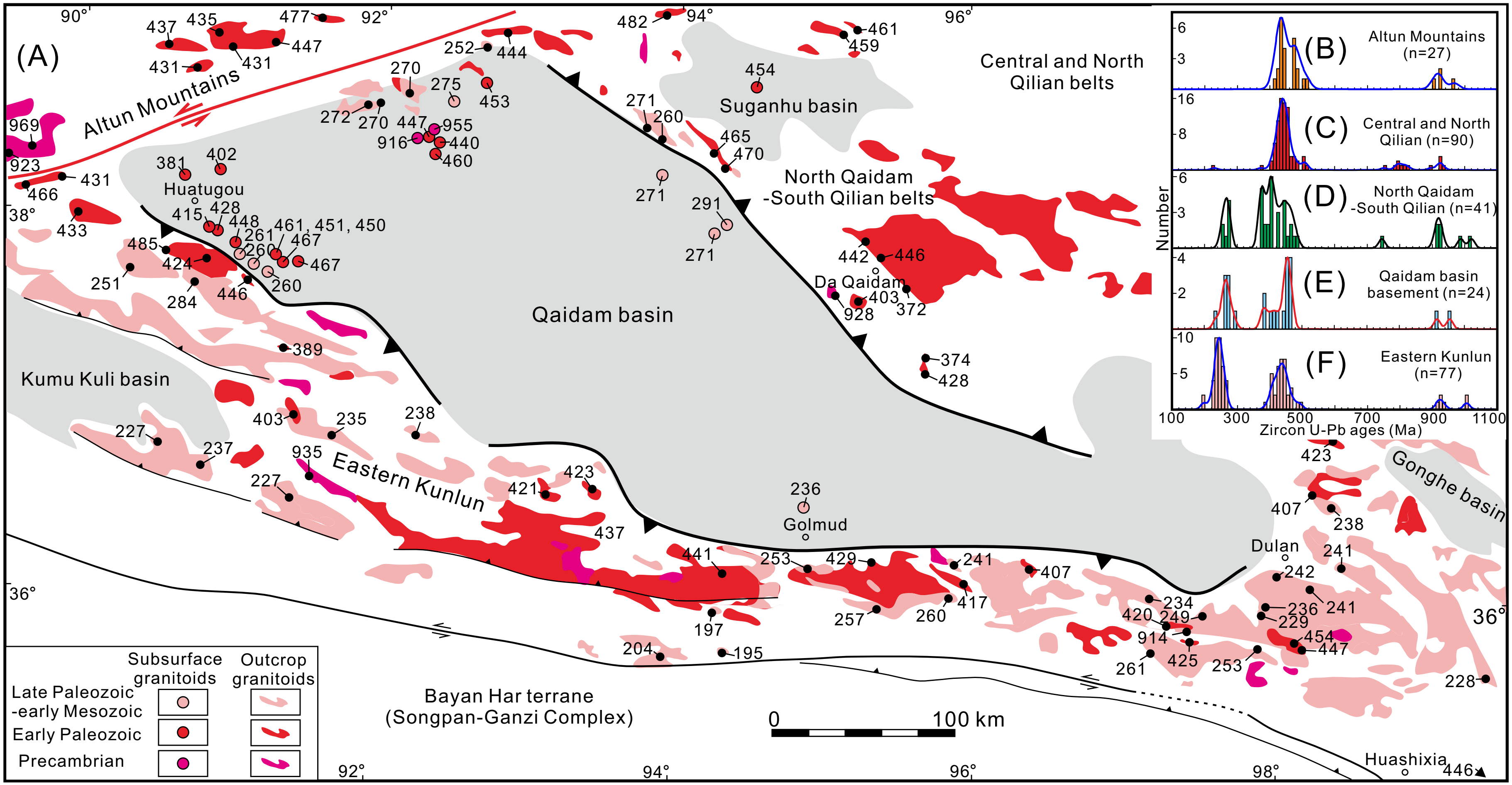

Fig. 6. Published zircon U-Pb ages of granitoids in northern Tibet. (A) Representative ages showing on the map. (B–F) Granitoid zircon age KDE plots for the Altun Mountains (B), Central and North Qilian belts (C), North Qaidam-South Qilian belts (D), Eastern Kunlun (F) and the subsurface basement of the Qaidam basin (E). The data of the Central and North Qilian belts were summarized by Zhang et al. (in preparation); the other data are summarized in this study (Table S3 in the Supplement materials). Note that these three regions experienced similar subduction-collision-related magmatic histories with three major stages at early Neoproterozoic (ca. 900–1000 Ma), latest Cambrian to Middle Devonian (ca. 375–490 Ma) and Permian to Triassic (ca. 220–275 Ma). The zircon age data are from Cowgill et al. (2003); Gehrels et al. (2003b); Meng et al. (2005); Wu et al., 2007a, 2008, 2014a, 2014b; Guo et al. (2011); Chen et al., 2012, 2015, 2016a; Liu et al. (2012, 2014); Wang et al. (2012b, 2014); Xiong et al. (2012, 2014, 2015); Dai et al. (2013); Li et al. (2013, 2015a,b); Dong et al. (2015); Zhou et al. (2016); Cheng et al. (2017); Shao et al. (2017); Gao et al. (2018); He et al. (2018) and references therein; Lu et al. (2018) and references therein; Wang et al. (2018); Zheng et al. (2018).

were proposed to be deposited under passive margin settings (Wu et al., 2019b), a relatively long-distance sediment supply from a far source region with similar early–middle Neoproterozoic magmatism signatures also cannot be excluded.

The detrital zircons in the upper Paleozoic strata display overwhelming early Paleozoic ages (Fig. 4), matching with the widespread late Cambrian–early Devonian arc-related granitoids in Kunlun-Qaidam terrane and surrounding regions (Fig. 6). Thus, these zircon crystals are preferred to be derived from the nearby Proto-Tethys (also named as Paleo-Kunlun in some literatures) arc rocks (Dai et al., 2013; Li et al., 2013; Cheng et al., 2017; Dong et al., 2018; Wu et al., 2019a, 2019b, 2019c). The subordinate Neoproterozoic zircons in these upper Paleozoic samples (e.g., 14AX-48) have similar ages with the ones in those Neoproterozoic samples, revealing either recycling from the Neoproterozoic sedimentary strata or sharing the same sources with the Neoproterozoic sedimentary successions.

5.3. Affinity and Precambrian evolution of the Eastern Kunlun

Figs. 7A and 8A illustrate zircon age kernel density estimation (KDE) and non-metric multi-dimensional scaling (MDS) plots, respectively, for comparison of the Precambrian basement detrital zircon U-Pb age populations of the Eastern Kunlun Range and the surrounding regions (including North China, Tarim, Yangtze, Cathaysia blocks, Qiangtang, Qinling and Qilian terranes, Fig. 1A). Given that all the Precambrian sedimentary rocks from the Eastern Kunlun Range, the North Qaidam metamorphic belt and the Qilian terrane show high zircon U-Pb age probabilities of 700–1000 Ma (Fig. 7 and references therein); and the Qilian terrane was a potential source for the Eastern Kunlun Neoproterozoic sedimentary strata, as above proposed, we suggest that the Kunlun-Qaidam and Qilian terranes were probably within a single tectonic domain during the Neoproterozoic, at odds with the idea of these 'terranes' as separate micro-continents during the Neoproterozoic. We herein refer to this undifferentiated tectonic domain as the Kunlun-Qaidam-Qilian (KQQ) block. This hypothesis is also supported with previous petrology, geochemistry and geochronology studies on granitoids therein (Fig. 6) which conclude that contemporaneous magmatism with same or similar origin and source nature (most S-type and I-type granites) prevailed in these 'terranes' during the early Neoproterozoic (0.9–1.0 Ga) (He et al., 2018 and reference therein). The early Neoproterozoic magmatic and metamorphic events in the KQQ block are generally proposed as later stages of the global

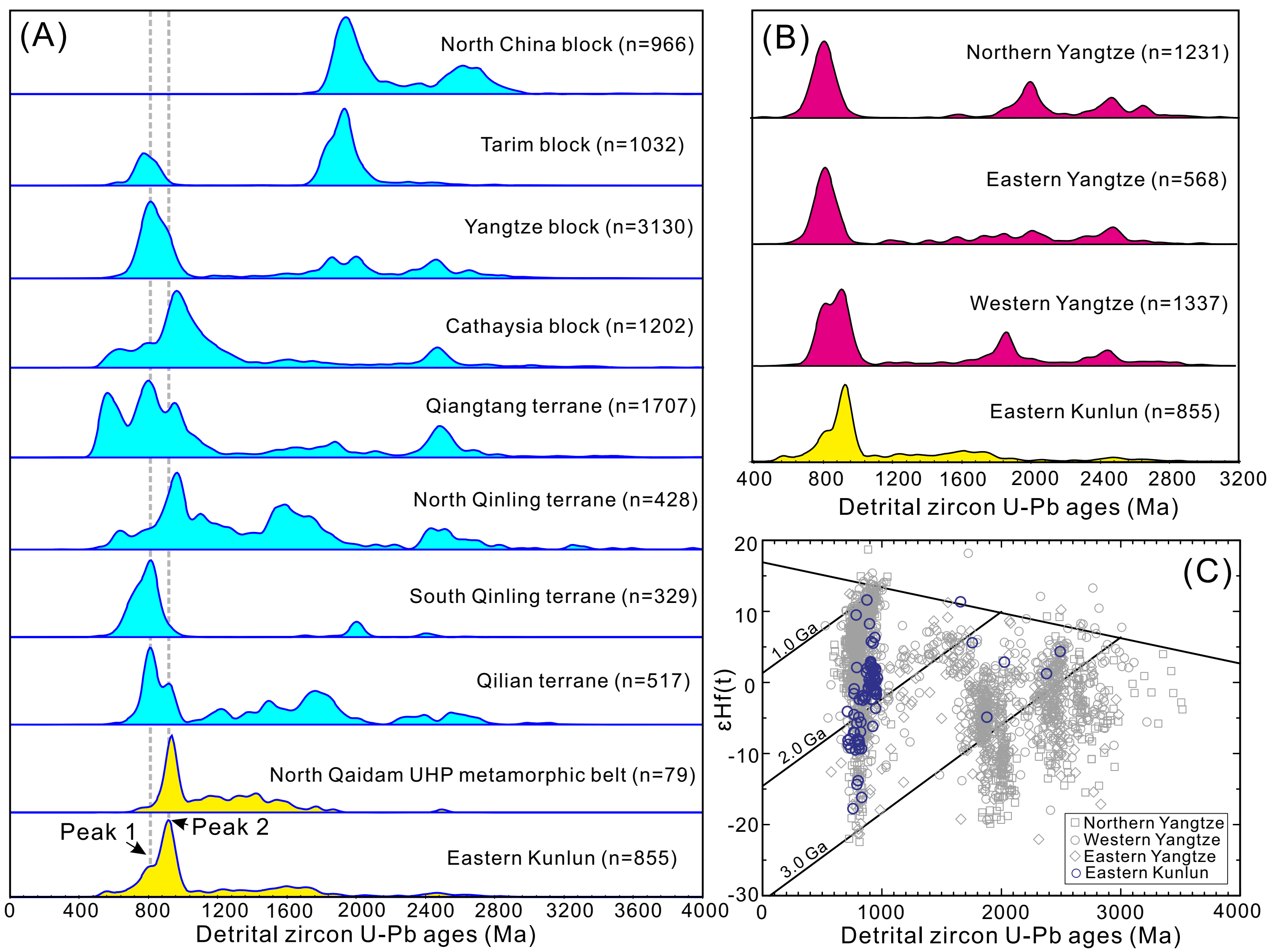

Fig. 7. Comparison of Precambrian detrital zircon U-Pb ages (A, B) and Hf isotopes (C) of the Eastern Kunlun and the surrounding blocks or terranes. Note that the analyzed samples of the Eastern Kunlun in this study show two different Neoproterozoic detrital zircon age populations, with the peak ages at ~920 Ma and ~800 Ma. Data of the North China block are from Darby and Gehrels (2006); Xia et al. (2006a,b) and Tung et al. (2007b). Data of the Tarim block are from Gehrels et al. (2011); Zhu et al. (2011a); Carroll et al. (2013) and Xu et al., 2013b. Data of the Yangtze block are from Liu et al. (2008); Sun et al. (2008, 2009); Wang et al., 2010, 2012a, 2013. Data of the Cathaysia block are from Yu et al. (2008); Yao et al. (2011, 2014). Data of the Qiangtang terrane are from Pullen et al. (2008); Gehrels et al. (2011) and He et al. (2011). Data of the North Qinling terrane are from Diwu et al. (2010); Wan et al. (2011) and Zhu et al. (2011b). Data of the South Qinling terrane are from Ling et al. (2010). Data of the Qilian terrane are from Tung et al. (2007a); Xu et al. (2007) and Gehrels et al. (2011). Data of the Eastern Kunlun are from this study (samples 13SG-158, 14AX-12, 14AX-15 and 14AX-26) and the following references: Chen et al. (2011); He et al., 2016a, 2016b; Meng et al. (2017) and Yan et al. (2017).

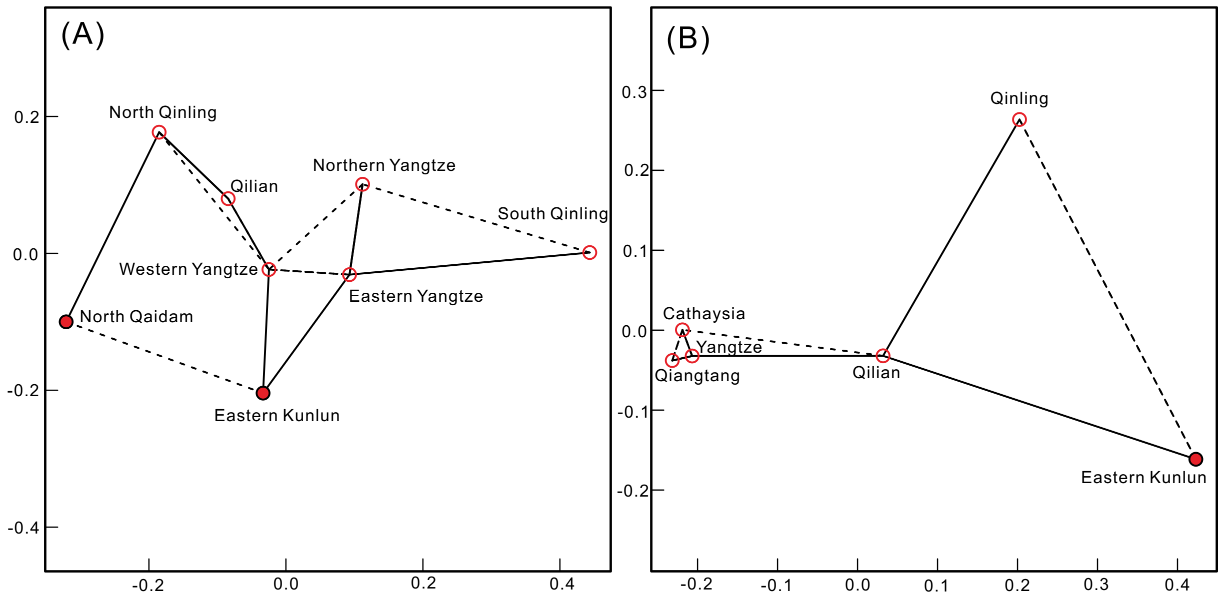

Fig. 8. Non-metric multi-dimensional scaling (MDS) plots for detrital zircon U-Pb age comparison among the Eastern Kunlun and the surrounding blocks (A: Precambrian sedimentary rocks; B: Paleozoic sedimentary rocks). The R programming language-based Provenance software (Vermeesch et al., 2016) was employed for the illustration. Solid lines and dashed lines indicate the closest and second closest neighbors, respectively.

Grenvillian orogenesis, recording the amalgamation of the supercontinent Rodinia (Song et al., 2012; Yu et al., 2013, 2019b; Wang et al., 2016b; Cheng et al., 2017; He et al., 2018).

The North China block is known to have Archean and Paleoproterozoic basement rocks (Darby and Gehrels, 2006; Xia et al., 2006a,b; Tung et al., 2007b), with major zircon age probability peaks at 2.5–2.6 Ga and 1.8–2.0 Ga (Fig. 7A). The Tarim block is characterized by Paleoproterozoic and Neoproterozoic basement rocks (Gehrels et al., 2011; Zhu et al., 2011a; Carroll et al., 2013; Xu et al., 2013b), and has dominant zircon age populations of 1.8–2.0 Ga and 700–900 Ma (Fig. 7A). The Qiangtang terrane, which is considered to have Gondwana-affinity, contains Neoproterozoic basement but with significant "Pan-African" (550–650 Ma) and Grenvillian (980–1200 Ma) zircons (Fig. 7A; Pullen et al., 2008; Gehrels et al., 2011; He et al., 2011). Our new data indicate distinct detrital zircon age distributions of the analyzed samples from the zircon age populations of these three blocks (Fig. 7). Hence, the KQQ block is interpreted to have a disparate history with these three blocks during the Neoproterozoic.

We favor that the KQQ block had affinity with the South China block. The South China block, which was formed due to the collision and amalgamation of the Yangtze and Cathaysia blocks, is widely thought to have been part of the Rodinia supercontinent during the Neoproterozoic (e.g., Li et al., 2008; Yu et al., 2008; Cawood et al., 2013). Note that the basement of Cathaysia block has significant Grenvillian (950–1100 Ma) zircons (e.g., Yu et al., 2008; Yao et al., 2011, 2014), whereas the Yangtze block basement is characterized by 750–1000 Ma zircons (Liu et al., 2008; Sun et al., 2008, 2009; Wang et al., 2010, 2012a,b, 2013), similar to the basement zircon age populations of the KQQ block (Figs. 7–8). The Yangtze-affinity of the KQQ block is also reinforced by the Neoproterozoic detrital zircon Hf isotopic data which indicate εHf(t) values ranging ca. −20–10 for both the KQQ block and Yangtze block (He et al., 2018 and reference therein; Fig. 7C). We further infer that the KQQ block was most likely linked to the western Yangtze block (Fig. 9), since the middle–late Neoproterozoic basement rocks within the western Yangtze block are dominated by zircon age peaks of ~920 Ma and ~800 Ma (Zhou et al., 2006; Sun et al., 2008, 2009; Wang et al., 2012a), whereas the contemporaneous rocks within the northern and eastern Yangtze block typically yield probability age peaks at ~820 Ma (Fig. 7B). The highly consistent Neoproterozoic stratigraphic and lithological assemblages in the Eastern Kunlun, North Qaidam, Central Qilian and Western Yangtze regions (Fig. 9C; Li et al., 2002; Ling et al., 2003; Shen et al., 2003; Yang et al., 2009) and those widely spread ca. 0.9–1.0 Ga granitic rocks in the regions (Fig. 6) also support the Neoproterozoic association between the western Yangtze and the KQQ blocks. Here, we refer to the combined continent of the KQQ block and the South China block as Greater South China block (Fig. 9).

Note that previous intensive tectono-magmatic history comparative studies between the South China block and other blocks in Rodinia supercontinent suggested that the South China block was most likely linked with the northern Greater India, West Australia and East Antarctica continents (Yu et al., 2008; Wang et al., 2012a; Cawood et al., 2013; Zhao et al., 2018 and references therein). Furthermore, the above-mentioned pervasive early Neoproterozoic (i.e., ca. 0.9–1.0 Ga) magmatic events in the Eastern Kunlun, Qaidam, Qilian and western Yangtze regions are generally inferred to be the result of a continental convergent margin setting (e.g., Ling et al., 2003; Shen et al., 2003; Yang et al., 2009; Yu et al., 2013; Cheng et al., 2017; He et al., 2018). If valid, this would place the Greater South China block along northwest margin of the Rodinia (Fig. 9, Fig. 10A), rather than within the supercontinental interior. This posit also agrees with proposed long-lived east and north verging (present-day orientation) subduction and arc magmatic system along the margin of the Yangtze block during the early Neoproterozoic (Fig. 9A; Zhou et al., 2002, 2006; Sun et al., 2008; Yu et al., 2008; Wang et al., 2012a; Cawood et al., 2013; Zhang et al., 2017a; Li et al., 2018a).

Previous studies on Paleozoic sedimentary strata in the South China block indicate obvious Pan-African zircon age signatures (ca. 550–650 Ma, marking the assembly of the supercontinent Gondwana), implying that the South China block was linked to the Gondwana during most periods of the Paleozoic (Duan et al., 2011; Cawood et al., 2013; Xu et al., 2013a; Chen et al., 2016b), whereas the Pan-African zircon age signature is rare in the analyzed Paleozoic samples from the Eastern Kunlun (Fig. 4). Therefore, we favor that the KQQ block was most likely separated from the Greater South China block before feeding of the Pan-African belts-sourced detritus, i.e., before ca. 550–650 Ma (Fig. 10B).

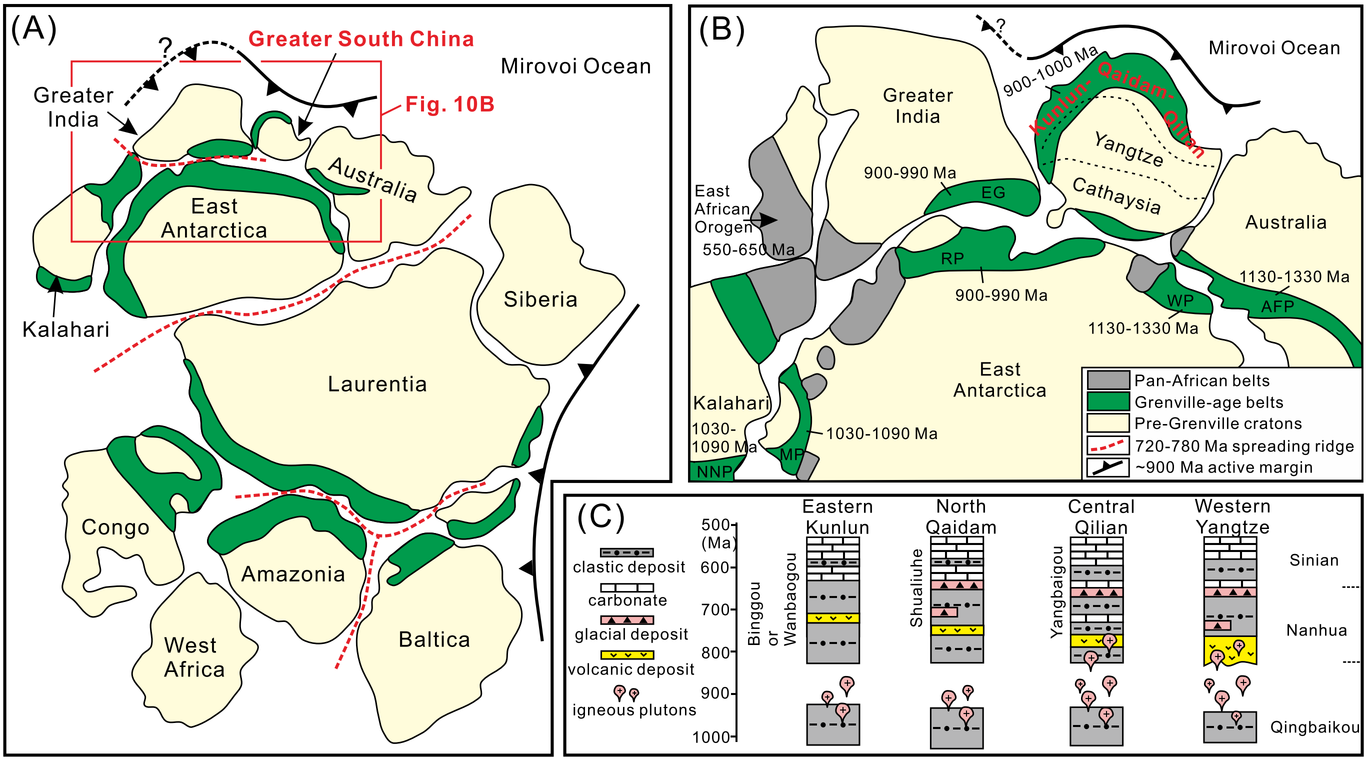

Fig. 9. Position of the Greater South China block (A) and the KQQ block (B) in the early Neoproterozoic (ca. 900 Ma) Rodinia supercontinent, modified from Hoffman (1991), Fitzsimons (2000), Li et al. (2008) and Yu et al. (2008). (C) Neoproterozoic tectonostratigraphic correlations between Eastern Kunlun, North Qaidam, Central Qilian and Western Yangtze regions (modified from Li et al. (1996); Pan et al. (2004); Tung et al. (2007a) and Shen et al. (2010)). The Greater South China block is favored to be located on the margin of Rodinia, rather than inside the supercontinent (Yu et al., 2008; Wang et al., 2012a; Cawood et al., 2013; Zhao et al., 2018 and references therein). The KQQ block was likely separated from western Greater South China block prior to the formation of the Pan-African belts (ca. 550–650 Ma). The Kunlun-Qaidam terrane therein was probably close to the western Yangtze, whereas the Qilian terrane might be relatively close to the northern Yangtze, based on the interpretation of the zircon age MDS plots (Fig. 8). The details of the mentioned Grenvillian orogenic belts are as follows. NNP: Namaqua-Natal province; MP: Maud province; RP: Rayner province; EG: Eastern Ghats; WP: Wilkes province; AFP: Albany-Fraser province.

5.4. Paleozoic to Triassic subduction and accretion in the Eastern Kunlun and surrounding regions

Provenance interpretations for the Paleozoic samples (i.e. 14AX-35, 14AX-38, 14AX-48 and 14AX-51) from the Eastern Kunlun Range reveal that the Kunlun-Qaidam terrane was involved into a Paleozoic tectono-magmatic event after separation from the Rodinia, i.e., late Cambrian to Middle–Late Devonian (380–500 Ma). Previous detrital zircon geochronology studies indicate dominant 400–500 Ma and 230–290 Ma zircons in the Mesozoic–Cenozoic sedimentary rocks and modern river sands relative to the Eastern Kunlun Range (e.g., Ding et al., 2013; Li et al., 2013; Cheng et al., 2016; Jian et al., 2019a), and thus proves the existence of late Cambrian–Devonian and Permian–Triassic tectono-magmatic episodes. Taking into account the published geochronology results of granitoid rocks in the Eastern Kunlun Range (Fig. 6 and reference therein), the second episode (mainly during the Permian–Triassic) could be extended to earliest Jurassic time (ca. 195 Ma). These two episodes are generally interpreted as the results of successive subductions of Proto-Tethys (430–500 Ma) and Paleo-Tethys (230–290 Ma) oceans and subsequent continental collisions (Fig. 10C–E; Dai et al., 2013; Li et al., 2013; Cheng et al., 2017; Dong et al., 2018).

It is worth noting that the late Cambrian–Devonian and Permian–Triassic granitoid rocks are widespread but spatially varied in northern Tibet (Fig. 6). Although late Cambrian–Devonian granitoids are present in all the terranes, those Eastern Kunlun and Qaidam granitoids are thought to be linked to melting of a continental crust, whereas those Qilian granitoids are regarded to be derived from Paleo/Mesoproterozoic basement rocks with significant involvement of mantle-derived materials (Cheng et al., 2017 and reference therein). This implies that the late Cambrian–Devonian granitoids in northern Tibet were probably generated by distinct subduction and collision zones (Fig. 10C). Although the late Cambrian–Devonian history of the North Qaidam and North Qilian metamorphic belts remain highly controversial (e.g., existence or absence of an oceanic subduction in the North Qaidam region and subduction directions of the Qilian ocean) (e.g., Yang et al., 2002a, b; Gehrels et al., 2003a,b; Yin et al., 2007; Song et al., 2013, 2014; Cheng et al., 2017), recently, a growing number of evidence suggests that subduction, collision and magmatism zones prevailed along the Eastern Kunlun, North Qaidam and North Qilian belts during the early Paleozoic and south-dipping subduction of the Qilian ocean occurred along the North Qilian belt (Song et al., 2017, 2018, 2019; Zhang et al., 2017c; Dong et al., 2018; Mu et al., 2018; Zuza et al., 2018; Wu et al., 2019a,b,c; Yang et al., 2019; Yu et al., 2019a,c). Absence of Permian–Triassic granitoid rocks (Fig. 6) may indicate that most of the Qilian block was not involved in the Paleo-Tethys subduction system (Song et al., 2013). By contrast, the 200–290 Ma granitoid rocks are widespread in the Eastern Kunlun and Qaidam regions (Fig. 6). This implies that the Permian–Triassic subduction of the Paleo-Tethys ocean did not only occur in the Eastern Kunlun region, but also influenced the entire Qaidam block to the north (>300 km), as far as the region of the North Qaidam and South Qilian metamorphic belts (Fig. 10E).

5.5. A summary of the Neoproterozoic–Paleozoic tectonic evolution of the northern Tibet

A synthesis of the new data and previously published data of sedimentary and igneous rocks demonstrates that three epochs of subduction-collision-related orogeneses, i.e., early–middle Neoproterozoic, late Cambrian–Devonian and Permian–Triassic, are

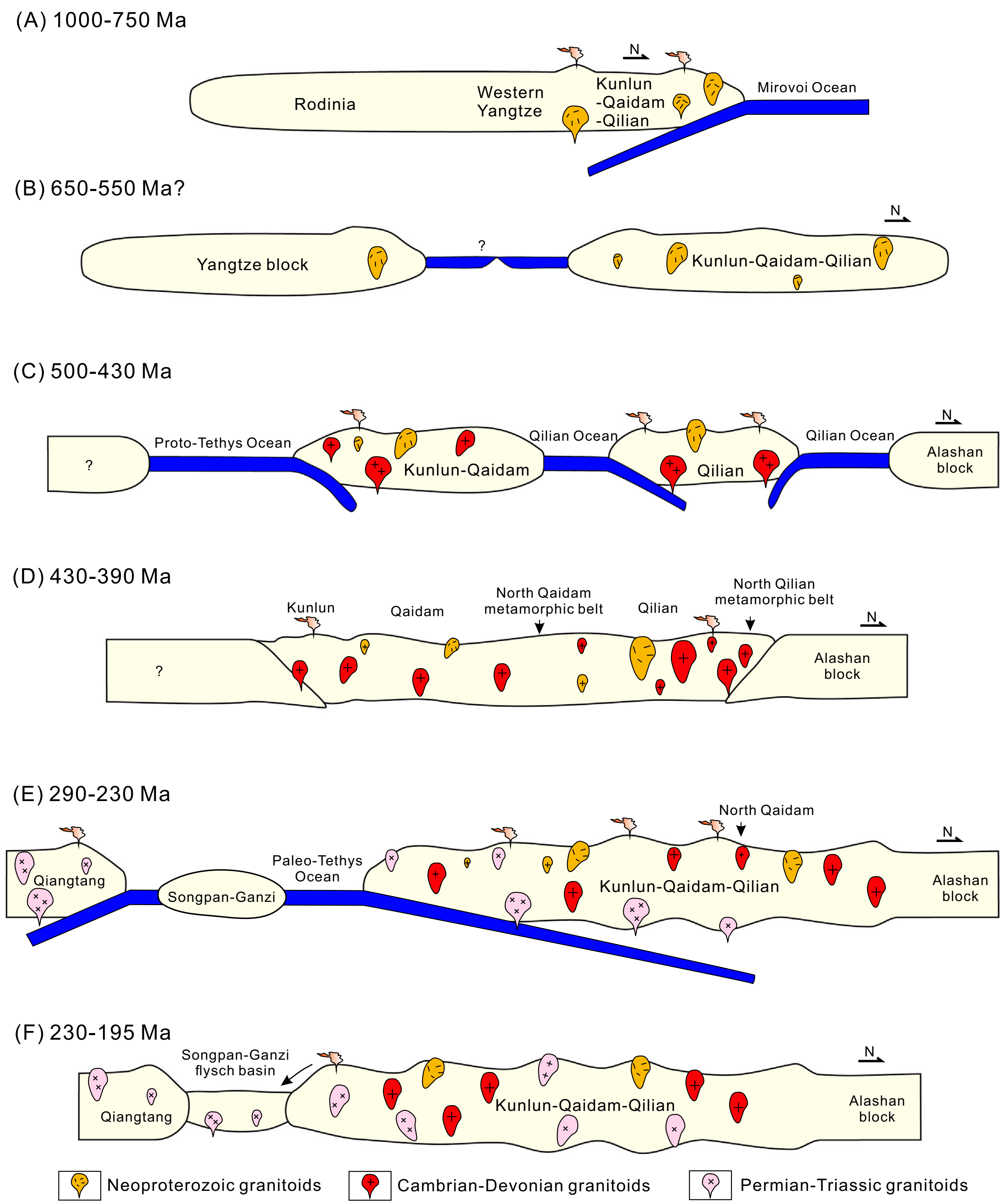

Fig. 10. A sketched model illustrating Neoproterozoic evolution and Paleozoic to Triassic subduction and accretionary history of the Eastern Kunlun and surrounding regions in northern Tibet. Refer to the Section 5.5 for the details.

involved in northern Tibet. A six-stage tectonic evolution model for the Neoproterozoic–Paleozoic northern Tibet is illustrated in Fig. 10 and is briefly stated as follows.

1) The Kunlun-Qaidam and Qilian terranes, as a single tectonic domain (named as the Kunlun-Qaidam-Qilian block), connected with the western Yangtze block, forming the Greater South China block, and were most likely located in an active margin of the Rodinia supercontinent during the early–middle Neoproterozoic (Fig. 10A). Deposition of this period in the Eastern Kunlun region is characterized by arc-related sedimentary succession interbedded by volcanic or volcaniclastic rocks.
2) The Kunlun-Qaidam-Qilian block was separated from the Greater South China block prior to the period of Pan-African orogenesis (ca. 550–650 Ma, Fig. 10B). Deposition of this period in the Eastern Kunlun region was likely in a passive continental margin (extensional) setting and formed those shallow marine mixed carbonate-siliciclastic sedimentary successions.
3) North-dipping Proto-Tethys oceanic subduction occurred at the southern margin of the Kunlun-Qaidam terrane during the

Cambrian to middle Silurian (Fig. 10C). At the same time, the Qilian block was sandwiched by South Qilian and North Qilian arcs, due to the Qilian ocean northward and southward subduction events (Zuza et al., 2018; Yang et al., 2019), respectively.

4) Closure of the Proto-Tethys and Qilian oceans and collision of the micro-continents during the late Silurian to Middle Devonian, resulted in a coherent tectonic domain for the region of the northern Tibet (Fig. 10D). The North Qaidam ultra-high pressure metamorphic belt was generated by exhumation of the deeply subducted continental crust (Song et al., 2014; Yu et al., 2019a).
5) Low-angle, north-dipping subduction of the Paleo-Tethys ocean and associated arc magmatism impacted the whole Kunlun-Qaidam terrane during the Permian to Middle Triassic (Fig. 10E).
6) Uplift and exhumation of the Eastern Kunlun Range led to a major source of the Eastern Kunlun for the turbidite-dominated Songpan-Ganzi basin during the Late Triassic (Jian et al., 2019a; Fig. 10F). Subsequent closure of the Paleo-Tethys ocean and related magmatism initiated intensive deformation of the Songpan-Ganzi flysch successions (Pullen et al., 2008; Zhang et al., 2014).

6. Conclusions

This study conducts detrital zircon U-Pb geochronology and Hf isotope analysis of Proterozoic and Paleozoic metasedimentary rocks collected from the Eastern Kunlun Range and the North Qaidam metamorphic belt, compiles published detrital and igneous zircon age data of the northern Tibet, and yields the following conclusions.

1) The new detrital zircon age data indicate that most investigated Proterozoic strata were most likely deposited in the middle–late Neoproterozoic. The sedimentary strata of this period are wider spread in the region of northern Tibet than previously known. In addition, two analyzed metasedimentary rock outcrops, previously mapped as the Paleoproterozoic Baishahe Group, show dominant Paleozoic detrital zircon ages, highlighting that the Precambrian strata in the Eastern Kunlun Range deserve more attention in future study.
2) Provenance analysis results indicate that the middle–late Neoproterozoic sedimentary rocks in the Eastern Kunlun Range were likely sourced from both the Kunlun-Qaidam and Qilian terranes. This suggests that these terranes were within a single tectonic domain during the Neoproterozoic, rather than separated microcontinents. This connected continent was probably linked to the western Yangtze block, located in northwest margin of supercontinent Rodinia during the early–middle Neoproterozoic.
3) The Eastern Kunlun Range was involved into two tectono-magmatic episodes during the Phanerozoic, interpreted as the Proto-Tethys ocean subduction and collision in the late Cambrian–Devonian and the Paleo-Tethys ocean subduction and collision in the Permian–Triassic. In combination with published results and data of the granitoids in the northern Tibet, we favor that the Kunlun-Qaidam and Qilian terranes most likely underwent separated subduction and accretion process during the late Cambrian–Devonian, but together formed the upper plate to the northward subduction of the Paleo-Tethys ocean in the Permian–Triassic.

Declaration of competing interest

The authors declare that they have no known competing financial interests or personal relationships that could have appeared to influence the work reported in this paper.

Acknowledgments

This work was supported by the National Natural Science Foundation of China (No. 41806052), the Natural Science Foundation of Fujian Province (No. 2017J05067), Xiamen University Fundamental Research Funds for the Central Universities (Nos. 20720190097, 20720190103) and the National Science Foundation of US (EAR-1118908 and EAR-1118525). We appreciate Wei Zhang, Will Jackson Jr. and Delores Robinson for their assistance during the field work. George Gehrels, Mark Pecha, Nicky Giesler, Sonnet Gomes, Russ Linger, Jon Campbell and Sam Bowman are thanked for their help on the zircon U-Pb dating and Hf isotope analysis. We also appreciate Lin Li and other two anonymous reviewers for their helpful comments on the manuscript.

Appendix A. Supplementary data

Supplementary data to this article can be found online at https://doi.org/10.1016/j.gr.2020.01.015.

References

A, C., Wang, Y., Ren, J., Bao, G., 2003. Disintegration of the Wanbaogou Group and discovery of Early Cambrian strata in the East Kunlun area. Chinese Geology 30, 199–206 (In Chinese with English Abstract).

An, K., Lin, X., Wu, L., Cheng, X., Chen, H., Ding, W., Zhang, F., Gong, J., Yang, R., Zhu, K., Li, C., Zhang, Y., Gao, S., 2018. Reorganization of sediment dispersal in the Jiuxi Basin at ~17 Ma and its implications for uplift of the NE Tibetan Plateau. Palaeogeogr. Palaeoclimatol. Palaeoecol. 511, 558–576.

Bao, J., Wang, Y., Song, C., Feng, Y., Hu, C., Zhong, S., Yang, J., 2017. Cenozoic sediment flux in the Qaidam Basin, northern Tibetan Plateau, and implications with regional tectonics and climate. Glob. Planet. Chang. 155, 56–69.

Barbeau Jr., D.L., Ducea, M.N., Gehrels, G.E., Kidder, S., Wetmore, P.H., Saleeby, J.S., 2005. U-Pb detrital-zircon geochronology of northern Salinian basement and cover rocks. Geol. Soc. Am. Bull. 117, 466–481.

Bureau of Geology and Mineral Resources of Qinghai Province (BGMRQP), 1991. Regional Geology of Qinghai Province. Geological Publishing House, Beijing (In Chinese with English Abstract).

Carroll, A.R., Dumitru, T.A., Graham, S.A., Hendrix, M.S., 2013. An 800 million-year detrital zircon record of continental amalgamation: Tarim basin, NW China. Int. Geol. Rev. 55, 818–829.

Cawood, P.A., Wang, Y., Xu, Y., Zhao, G., 2013. Locating South China in Rodinia and Gondwana: a fragment of greater India lithosphere. Geology 41, 903–906.

Chen, N., Li, X., Zhang, K., Wang, G., Zhu, Y., Hou, G., Bai, Y., 2006. Lithological characteristics of the Baishahe Formation to the south of Xiangride Town, Eastern Kunlun Mountains and its age constrained from zircon Pb-Pb dating. Geological Science and Technology Information 25, 1–7 (In Chinese with English Abstract).

Chen, N.S., Xia, X.P., Li, X.Y., Sun, M., Xu, P., Liu, X.M., Wang, X.Y., Wang, Q.Y., 2007a. Timing of magmatism of the gneissic–granite plutons along north Qaidam margin and implications for Precambrian crustal accretions: zircon U-Pb dating and Hf isotope evidences. Acta Petrol. Sin. 23, 501–512 (In Chinese with English Abstract).

Chen, S., Li, R., Ji, W., Zhao, Z., Meng, Y., Shi, B., 2007b. The deposition characteristics and tectono-paleogeographic environment of Kunlun orogenic belt in Late Devonian. Geotecton. Metallog. 31, 44–51 (In Chinese with English Abstract).

Chen, Y., Pei, X., Li, R., Liu, Z., Li, Z., Zhang, X., Chen, G., Liu, Z., Ding, S., Guo, J., 2011. Zircon U-Pb age of Xiaomiao Formation of Proterozoic in the eastern section of the East Kunlun orogenic belt. Geoscience 25, 510–521 (In Chinese with English Abstract).

Chen, X., Gehrels, G., Yin, A., Li, L., Jiang, R.B., 2012. Paleozoic and Mesozoic basement magmatisms of eastern Qaidam Basin, northern Qinghai-Tibet Plateau: LA-ICP-MS zircon U-Pb geochronology and its geological significance. Acta Geologica Sinica-English Edition 86, 350–369.

Chen, X., Gehrels, G., Yin, A., Zhou, Q., Huang, P., 2015. Geochemical and Nd–Sr–Pb–O isotopic constrains on Permo–Triassic magmatism in eastern Qaidam Basin, northern Qinghai-Tibetan plateau: implications for the evolution of the Paleo-Tethys. J. Asian Earth Sci. 114, 674–692.

Chen, J., Fu, L., Wei, J., Tian, N., Xiong, L., Zhao, Y., Zhang, Y., Qi, Y., 2016a. Geochemical characteristics of Late Ordovician granodiorite in Gouli area, Eastern Kunlun orogenic belt, Qinghai province: implications on the evolution of Proto-Tethys Ocean. Earth Sci. 41, 1863–1882 (In Chinese with English Abstract).

Chen, Q., Sun, M., Long, X., Zhao, G., Yuan, C., 2016b. U-Pb ages and Hf isotopic record of zircons from the late Neoproterozoic and Silurian–Devonian sedimentary rocks of the western Yangtze Block: implications for its tectonic evolution and continental affinity. Gondwana Res. 31, 184–199.

Cheng, F., Jolivet, M., Fu, S., Zhang, Q., Guan, S., Yu, X., Guo, Z., 2014. Northward growth of the Qimen Tagh Range: a new model accounting for the late Neogene strike-slip deformation of the SW Qaidam Basin. Tectonophysics 632, 32–47.

Cheng, F., Guo, Z., Jenkins, H.S., Fu, S., Cheng, X., 2015. Initial rupture and displacement on the Altyn Tagh fault, northern Tibetan Plateau: constraints based on residual Mesozoic to Cenozoic strata in the western Qaidam Basin. Geosphere 11, 921–942.

Cheng, F., Fu, S., Jolivet, M., Zhang, C., Guo, Z., 2016. Source to sink relation between the Eastern Kunlun Range and the Qaidam Basin, northern Tibetan Plateau, during the Cenozoic. Geol. Soc. Am. Bull. 128, 258–283.

Cheng, F., Jolivet, M., Hallot, E., Zhang, D., Zhang, C., Guo, Z., 2017. Tectono-magmatic rejuvenation of the Qaidam craton, northern Tibet. Gondwana Res. 49, 248–263.

Cheng, F., Garzione, C., Jolivet, M., Wang, W., Dong, J., Richter, F., Guo, Z., 2019a. Provenance analysis of the Yumen Basin and northern Qilian Shan: implications for the

pre-collisional paleogeography in the NE Tibetan plateau and eastern termination of Altyn Tagh fault. Gondwana Res. 65, 156–171.
Cheng, F., Jolivet, M., Guo, Z., Lu, H., Zhang, B., Li, X., Zhang, D., Zhang, C., Zhang, H., Wang, L., Wang, Z., Zhang, Q., 2019b. Jurassic–Early Cenozoic tectonic inversion in the Qilian Shan and Qaidam Basin, North Tibet: new insight from seismic reflection, isopach mapping and drill core data. J. Geophys. Res. Solid Earth https://doi.org/10.1029/2019JB018086.
Clark, M.K., Farley, K.A., Zheng, D., Wang, Z., Duvall, A.R., 2010. Early Cenozoic faulting of the northern Tibetan Plateau margin from apatite (U–Th)/He ages. Earth Planet. Sci. Lett. 296, 78–88.
Coutts, D.S., Matthews, W.A., Hubbard, S.M., 2019. Assessment of widely used methods to derive depositional ages from detrital zircon populations. Geosci. Front. 10, 1421–1435.
Cowgill, E., Yin, A., Harrison, T.M., Xiao-Feng, W., 2003. Reconstruction of the Altyn Tagh fault based on U-Pb geochronology: role of back thrusts, mantle sutures, and heterogeneous crustal strength in forming the Tibetan Plateau. Journal of Geophysical Research-Solid Earth 108, 2346. https://doi.org/10.1029/2002JB002080.
Dai, J., Wang, C., Hourigan, J., Santosh, M., 2013. Multi-stage tectono-magmatic events of the Eastern Kunlun Range, northern Tibet: insights from U-Pb geochronology and (U-Th)/He thermochronology. Tectonophysics 599, 97–106.
Darby, B.J., Gehrels, G., 2006. Detrital zircon reference for the North China Block. J. Asian Earth Sci. 26, 637–648.
Dickinson, W.R., Gehrels, G.E., 2009. Use of U-Pb ages of detrital zircons to infer maximum depositional ages of strata: a test against a Colorado Plateau Mesozoic database. Earth Planet. Sci. Lett. 288, 115–125.
Ding, L., Yang, D., Cai, F.L., Pullen, A., Kapp, P., Gehrels, G.E., Zhang, L.Y., Zhang, Q.H., Lai, Q.Z., Yue, Y.H., Shi, R.D., 2013. Provenance analysis of the Mesozoic Hoh-Xil-Songpan-Ganzi turbidites in northern Tibet: implications for the tectonic evolution of the eastern Paleo-Tethys Ocean. Tectonics 32. https://doi.org/10.1002/tect.20013.
Diwu, C.R., Sun, Y., Liu, L.A., Zhang, C.L., Wang, H.L., 2010. The disintegration of Kuanping Group in North Qinling orogenic belts and Neo-proterozoic N-MORB. Acta Petrol. Sin. 26, 2025–2038.
Dong, Y., Santosh, M., 2016. Tectonic architecture and multiple orogeny of the Qinling Orogenic Belt, Central China. Gondwana Res. 29, 1–40.
Dong, Y., Zhang, G., Neubauer, F., Liu, X., Genser, J., Hauzenberger, C., 2011. Tectonic evolution of the Qinling orogen, China: review and synthesis. J. Asian Earth Sci. 41, 213–237.
Dong, Z., Gu, P., Chen, R., Zhang, X., Zhang, H., 2015. Geochronology, geochemistry, and Hf isotoe of Yanchangbeishan adamellite of Lenghu Area in Qinghai. Earth Science (Journal of China University of Geosciences) 40, 130–144 (In Chinese with English Abstract).
Dong, Y., He, D., Sun, S., Liu, X., Zhou, X., Zhang, F., Yang, Z., Cheng, B., Zhao, G., Li, J., 2018. Subduction and accretionary tectonics of the East Kunlun orogen, western segment of the Central China Orogenic System. Earth Sci. Rev. 186, 231–261.
Duan, L., Meng, Q.R., Zhang, C.L., Liu, X.M., 2011. Tracing the position of the South China block in Gondwana: U–Pb ages and Hf isotopes of Devonian detrital zircons. Gondwana Res. 19, 141–149.
Fitzsimons, I.C.W., 2000. Grenville-age basement provinces in East Antarctica: evidence for three separate collisional orogens. Geology 28, 879–882.
Gao, G., Li, B., Yang, B., Liao, Y., 2018. Zircon U-Pb geochronology, geochemistry and Hf isotopic of granite porphyry in Xitieshan area of north margin of Qaidam basin. Global Geology 37, 747–760 (In Chinese with English Abstract).
Gehrels, G., Pecha, M., 2014. Detrital zircon U-Pb geochronology and Hf isotope geochemistry of Paleozoic and Triassic passive margin strata of western North America. Geosphere 10, 49–65.
Gehrels, G., Yin, A., Wang, X., 2003a. Detrital-zircon geochronology of the northeastern Tibetan Plateau. Geol. Soc. Am. Bull. 115, 881–896.
Gehrels, G., Yin, A., Wang, X.F., 2003b. Magmatic history of the northeastern Tibetan Plateau. Journal of Geophysical Research-Solid Earth 108, 1–14. https://doi.org/10.1029/2002jb001876.
Gehrels, G., Valencia, V., Pullen, A., 2006. Detrital zircon geochronology by laser-ablation multicollector ICPMS at the Arizona LaserChron Center. The Paleontological Society Paper 12, 67–76.
Gehrels, G., Kapp, P., DeCelles, P., Pullen, A., Blakey, R., Weislogel, A., Ding, L., Guynn, J., Martin, A., McQuarrie, N., Yin, A., 2011. Detrital zircon geochronology of pre-Tertiary strata in the Tibetan-Himalayan orogen. Tectonics 30, TC5016. https://doi.org/10.1029/2011TC002868.
Guo, T., Liu, R., Chen, F., Bai, X., Li, H., 2011. LA-MC-ICPMS zircon U-Pb dating of Wulanwuzhuer porphyritic syenite granite in the North Qimantagh belt mountain of Qinghai and its geological significance. Geological Bulletin of China 30, 1203–1211 (In Chinese with English Abstract).
Hacker, B.R., Ratschbacher, L., Liou, J.G., 2004. Subduction, collision and exhumation in the ultrahigh-pressure Qinling-Dabie orogen. Geol. Soc. Lond., Spec. Publ. 226, 157–175.
He, D.F., Dong, Y.P., Zhang, F.F., Yang, Z., Sun, S.S., Cheng, B., Zhou, B., Liu, X.M., 2016b. The 1.0 Ga S–type granite in the East Kunlun Orogen, Northern Tibetan Plateau: implications for the Meso- to Neoproterozoic tectonic evolution. J. Asian Earth Sci. 130, 46–59.
He, S., Li, R., Wang, C., Zhang, H., Ji, W., Yu, P., Gu, P., Shi, C., 2011. Discovery of ~4.0 Ga detrital zircons in the Changdu Block, North Qiangtang, Tibetan Plateau. Chin. Sci. Bull. 56, 647–658.
He, D.F., Dong, Y.P., Liu, X.M., Yang, Z., Sun, S.S., Cheng, B., Li, W., 2016a. Tectono-thermal events in East Kunlun, Northern Tibetan Plateau: evidence from zircon U-Pb geochronology. Gondwana Res. 30, 179–190.
He, D., Dong, Y., Liu, X., Zhou, X., Zhang, F., Sun, S., 2018. Zircon U–Pb geochronology and Hf isotope of granitoids in East Kunlun: implications for the Neoproterozoic magmatism of Qaidam Block, Northern Tibetan Plateau. Precambrian Res. 314, 377–393.
Hoffman, F.P., 1991. Did breakout of Laurentia turn Gondwana inside–out. Science 252, 1409–1411.
Hsu, K.J., Guitang, P., Sengor, A.M.C., 1995. Tectonic evolution of the Tibetan plateau: a working hypothesis based on the archipelago model of orogenesis. Int. Geol. Rev. 37, 473–508.
Hu, Y., Niu, Y., Li, J., Ye, L., Kong, J., Chen, S., Zhang, Y., Zhang, G., 2016. Petrogenesis and tectonic significance of the late Triassic mafic dikes and felsic volcanic rocks in the East Kunlun Orogenic Belt, Northern Tibet Plateau. Lithos 245, 205–222.
Huang, H., Niu, Y.L., Nowell, G., Zhao, Z.D., Yu, X.H., Mo, X.X., 2015. The nature and history of the Qilian Block in the context of the development of the Greater Tibetan Plateau. Gondwana Res. 28, 209–224.
Jian, X., Guan, P., Zhang, D.-W., Zhang, W., Feng, F., Liu, R.-J., Lin, S.-D., 2013a. Provenance of Tertiary sandstone in the northern Qaidam basin, northeastern Tibetan plateau: integration of framework petrography, heavy mineral analysis and mineral chemistry. Sediment. Geol. 290, 109–125.
Jian, X., Guan, P., Zhang, W., Feng, F., 2013b. Geochemistry of Mesozoic and Cenozoic sediments in the northern Qaidam basin, northeastern Tibetan plateau: implications for provenance and weathering. Chem. Geol. 360, 74–88.
Jian, X., Guan, P., Fu, S.T., Zhang, D.W., Zhang, W., Zhang, Y.S., 2014. Miocene sedimentary environment and climate change in the northwestern Qaidam basin, northeastern Tibetan Plateau: facies, biomarker and stable isotopic evidences. Palaeogeogr. Palaeoclimatol. Palaeoecol. 414, 320–331.
Jian, X., Guan, P., Zhang, W., Liang, H., Feng, F., Fu, L., 2018. Late Cretaceous to early Eocene deformation in the northern Tibetan plateau: detrital apatite fission track evidences from northern Qaidam basin. Gondwana Res. 60, 94–104.
Jian, X., Weislogel, A., Pullen, A., 2019a. Triassic sedimentary filling and closure of the Eastern Paleo-Tethys Ocean: new insights from detrital zircon geochronology of Songpan-Ganzi and Yidun flysch in Eastern Tibet. Tectonics 38, 767–787.
Jian, X., Zhang, W., Liang, H., Guan, P., Fu, L., 2019b. Mineralogy, petrography and geochemistry of an early Eocene weathering profile on basement granodiorite of Qaidam basin, northern Tibet: tectonic and paleoclimatic implications. Catena 172, 54–64.
Jolivet, M., Brunel, M., Seward, D., Xu, Z., Yang, J., Roger, F., Tapponnier, P., Malavieille, J., Arnaud, N., Wu, C., 2001. Mesozoic and Cenozoic tectonics of the northern edge of the Tibetan plateau: fission-track constraints. Tectonophysics 343, 111–134.
Jones III, J.V., Connelly, J.N., Karlstrom, K.E., Williams, M.L., Doe, M.F., 2009. Age, provenance, and tectonic setting of Paleoproterozoic quartzite successions in the southwestern United States. Geol. Soc. Am. Bull. 121, 247–264.
Li, Z.X., Zhang, L., Powell, C.M., 1996. Positions of the East Asian cratons in the Neoproterozoic supercontinent Rodinia. Aust. J. Earth Sci. 43, 593–604.
Li, Z.X., Li, X.H., Zhou, H., Kinny, P.D., 2002. Grenvillian continental collision in south China: new SHIMP U–Pb zircon results and implications for the configuration of Rodinia. Geology 30, 163–166.
Li, Z.X., Bogdanova, S.V., Collins, A.S., Davidson, A., De Waele, B., Ernst, R.E., Fitzsimons, I.C.W., Fuck, R.A., Gladkochub, D.P., Jacobs, J., Karlstrom, K., Lu, S., Natapov, L.M., Pease, V., Piasarevsky, S.A., Thrane, K., Vernikovsky, V., 2008. Assembly, configuration, and break-up history of Rodinia: a synthesis. Precambrian Res. 160, 179–210.
Li, W., Neubauer, F., Liu, Y.J., Genser, J., Ren, S.M., Han, G.Q., Liang, C.Y., 2013. Paleozoic evolution of the North Qimantagh belth magmatic arcs, Eastern Kunlun Mountains: constraints from zircon dating of granitoids and modern river sands. J. Asian Earth Sci. 77, 183–202.
Li, L., Meng, Q., Pullen, A., Garzione, C.N., Wu, G., Wang, Y., Ma, S., Duan, L., 2014a. Late Permian–early Middle Triassic back-arc basin development in West Qinling, China. J. Asian Earth Sci. 87, 116–129.
Li, X., Yuan, W., Hao, N., Duan, H., Chen, X., Mo, X., Zhang, A., 2014b. Characteristics and tectonic setting of granite in Wulonggou area, East Kunlun Mountains. Global Geology 33, 275–288 (In Chinese with English Abstract).
Li, R., Pei, X., Li, Z., Pei, L., Liu, C., Chen, Y., Chen, G., Liu, Z., Yang, J., 2015a. Geochemistry and zircon U–Pb geochronology of granitic rocks in the Buqingshan tectonic mélange belt, northern Tibet Plateau, China and its implications for Prototethyan evolution. J. Asian Earth Sci. 105, 374–389.
Li, X., Huang, X., Luo, M., Dong, G., Mo, X., 2015b. Petrogenesis and geodynamic implications of the Mid-Triassic lavas from East Kunlun, northern Tibetan Plateau. J. Asian Earth Sci. 105, 32–47.
Li, J.Y., Wang, X.L., Gu, Z.D., 2018a. Early Neoproterozoic arc magmatism of the Tongmuliang Group on the northwestern margin of the Yangtze Block: implications for Rodinia assembly. Precambrian Res. 309, 181–197.
Ling, W., Gao, S., Zhang, B., Li, H., Liu, Y., Cheng, J., 2003. Neoproterozoic tectonic evolution of the northwestern Yangtze craton, South China: implications for amalgamation and break-up of the Rodinia Supercontinent. Precambrian Res. 122, 111–140.
Ling, W.L., Duan, R.C., Liu, X.M., Cheng, J.P., Mao, X.W., Peng, L.H., Liu, Z.X., Yang, H.M., Ren, B.F., 2010. U–Pb dating of detrital zircons from the Wudangshan Group in the South Qinling and its geological significance. Chin. Sci. Bull. 55, 2440–2448.
Liu, Y., Genser, J., Neubauer, F., Jin, W., Ge, X., Handler, R., Takasu, A., 2005. 40Ar/39Ar mineral ages from basement rocks in the Eastern Kunlun Mountains, NW China, and their tectonic implications. Tectonophysics 398, 199–224.
Liu, X.M., Gao, S., Diwu, C.R., Ling, W.L., 2008. Precambrian crustal growth of Yangtze craton as revealed by detrital zircon studies. Am. J. Sci. 308, 421–468.
Liu, B., Ma, C., Zhang, J., Xiong, F., Huang, J., Jiang, H., 2012. Petrogenesis of Early Devonian intrusive rocks in the east part of Eastern Kunlun Orogen and implication for Early Palaeozoic orogenic processes. Acta Petrol. Sin. 28, 1785–1807 (In Chinese with English Abstract).
Liu, Q., Meng, F., Li, S., Feng, H., Jia, L., Tian, G., 2016. Geochronology of zircon from the paragneiss of Kuhai Group in southern East Kunlun terrane. Acta Petrol. Mineral. 35, 469–483 (In Chinese with English Abstract).

Liu, G., Zhang, Y., Xue, J., Wu, G., Chen, Y., 2014. Zircon LA-ICPMS U-Pb dating and geochemistry of basement granites from north Kunlun faults zone, western Qaidam Basin and their geological implications. Acta Petrol. Sin. 30, 1615–1627 (In Chinese with English Abstract).

Lu, S.N., 2002. Precambrian Geology in Northern Tibetan Plateau. Geological Publishing House, Beijing, pp. 1–125 (In Chinese with English Abstract).

Lu, L., Wu, Z., Hu, D., Barosh, P., Hao, S., Zhou, C., 2010. Zircon U-Pb age for rhyolite of the Maoniushan Formation and its tectonic significance in the East Kunlun Mountains. Acta Petrol. Sin. 26, 1150–1158.

Lu, H., Ye, J., Guo, L., Pan, J., Xiong, S., Li, H., 2018. Towards a clarification of the provenance of Cenozoic sediments in the northern Qaidam Basin. Lithosphere 11, 252–272.

Luan, Y., Gong, S., Yue, W., Meng, L., 2011. Analysis on sedimentary environment and sequence stratigraphy of Binggou Group in Areli belt of Ruoqiang county in Xinjiang Uygur autonomous region. Shangdong Land Resources 27, 1–6 (In Chinese with English Abstract).

Mattern, F., Schneider, W., 2000. Suturing of the Proto- and Paleo-Tethys oceans in the western Kunlun (Xinjiang, China). J. Asian Earth Sci. 18, 637–650.

Meng, Q.R., Zhang, G.W., 2000. Geologic framework and tectonic evolution of the Qinling orogen, central China. Tectonophysics 323, 183–196.

Meng, F., Zhang, J., Yang, J., 2005. Tectono-thermal event of post-HP/UHP metamorphism in the Xitieshan area of the North Qaidam Mountains, western China: isotopic and geochemical evidence of granite and gneiss. Acta Petrol. Sin. 21, 45–56 (In Chinese with English Abstract).

Meng, F.C., Zhang, J.X., Cui, M.H., 2013. Discovery of early Paleozoic eclogite from the East Kunlun, western China, and its tectonic significance. Gondwana Res. 23, 825–836.

Meng, F.C., Cui, M.H., Wu, X.K., Ren, Y.F., 2015. Heishan mafic-ultramafic rocks in the Qimantag area of Eastern Kunlun, NW China: remnants of an early Paleozoic incipient island arc. Gondwana Res. 27, 745–759.

Meng, F.C., Jia, L.H., Ren, Y.F., Liu, Q., Duan, X.P., 2017. Magmatic and metamorphic events recorded in the gneisses of the Wenquan region, East Kunlun Mountains, Northwest China: evidence from the zircon U-Pb geochronology. Acta Petrol. Sin. 33, 3691–3709.

Mo, X.X., Luo, Z.H., Deng, J.F., Yu, X.H., Liu, C.D., Chen, H.W., Yuan, W.M., Liu, Y.H., 2007. Granitoids and crustal growth in the East-Kunlun orogenic belt. Geol. J. China Univ. 13, 403–414 (In Chinese with English Abstract).

Mu, D., Li, S., Wang, Q., Somerville, I., Wang, Y., Zhao, S., Li, X., Yu, S., Suo, Y., 2018. Early Paleozoic orocline in the Central China orogen. Gondwana Res. 63, 85–104.

Pan, G.T., Ding, J., Yao, D.S., Wang, L.Q., 2004. Geological Map of the Tibetan Plateau at a Scale of 1:1.5 M With Explanations. Chengdu Cartographic Publishing House, Chengdu, pp. 1–144 (In Chinese with English Abstract).

Pei, X., Li, R., Li, Z., Liu, C., Chen, Y., Pei, L., Liu, Z., Chen, G., Li, X., Wang, M., 2018. Composition feature and formation process of Buqingshan composite accretionary melange belt in southern margin of East Kunlun orogen. Earth Sci. 43, 4498–4520 (In Chinese with English Abstract).

Peng, Y., Ma, Y., Liu, C., Sun, J., Hu, Z., Mou, H., Zheng, C., 2016. SHRIMP zircon ages of the Daganggou volcanic rocks in the Eastern Kunlun orogenic belt and their implications. Geological Bulletin of China 35, 356–363 (In Chinese with English Abstract).

Pullen, A., Kapp, P., Gehrels, G.E., Vervort, J.D., Ding, L., 2008. Triassic continental subduction in central Tibet and Mediterranean-style closure of the Paleo-Tethys Ocean. Geology 36, 5351–5354.

Qi, X., Yang, J., Fan, X., Wang, B., 2018. Chronology and geochemistry of the dacite in the Maoniushan Formation in eastern part of the Eastern Kunlun orogen. Bull. Mineral. Petrol. Geochem. 37, 482–494 (In Chinese with English Abstract).

Shao, F., Niu, Y., Liu, Y., Chen, S., Kong, J., Duan, M., 2017. Petrogenesis of Triassic granitoids in the East Kunlun Orogenic Belt, northern Tibetan Plateau and their tectonic implications. Lithos 282, 33–44.

Shen, W., Gao, J., Xu, S.J., 2003. Formation age and geochemical characteristics of the Lengshuiqing body, Yanbian, Sichuan Province. Acta Petrol. Sin. 19, 27–37 (In Chinese with English Abstract).

Shen, B., Xiao, S., Zhou, C., Kaufman, A.J., Yuan, X., 2010. Carbon and sulfur isotope chemostratigraphy of the Neoproterozoic Quanji Group of the Chaidam Basin, NW China: basin stratification in the aftermath of an Ediacaran glaciation postdating the Shuram event? Precambrian Res. 177, 241–252.

Smith, A.D., 2006. The geochemistry and age of ophiolitic strata of the Xinglongshan Group: implications for the amalgamation of the Central Qilian belt. J. Asian Earth Sci. 28, 133–142.

Song, S.G., Su, L., Li, X.H., Niu, Y.L., Zhang, L.F., 2012. Grenvile-age orogenesis in the Qaidam-Qilian block: the link between South China and Tarim. Precambrian Res. 220–221, 9–22.

Song, S., Niu, Y., Su, L., Xia, X., 2013. Tectonics of the north Qilian orogen, NW China. Gondwana Res. 23, 1378–1401.

Song, S., Niu, Y., Su, L., Zhang, C., Zhang, L., 2014. Continental orogenesis from ocean subduction, continent collision/subduction, to orogen collapse, and orogen recycling: the example of the North Qaidam UHPM belt, NW China. Earth Sci. Rev. 129, 59–84.

Song, S., Yang, L., Zhang, Y., Niu, Y., Wang, C., Su, L., Gao, Y., 2017. Qi-Qin accretionary belt in Central China Orogen: accretion by trench jam of oceanic plateau and formation of intra-oceanic arc in the Early Paleozoic Qin-Qi-Kun Ocean. Sci. Bull. 62, 1035–1038.

Song, S., Bi, H., Qi, S., Yang, L., Allen, M.B., Niu, Y., Su, L., Li, W., 2018. HP-UHP metamorphic belt in the East Kunlun orogen: final closure of the Proto-Tethys Ocean and formation of the Pan-North-China continent. J. Petrol. 59, 2043–2060.

Song, S.G., Wu, Z.Z., Yang, L.M., Su, L., Xia, X.H., Wang, C., Dong, J.L., Zhou, C.A., Bi, H.Z., 2019. Ophiolite belts and evolution of the Proto-Tethys Ocean in the Qilian Orogen. Acta Petrol. Sin. 35, 2948–2970 (In Chinese with English Abstract).

Spencer, C.J., Kirkland, C.L., Taylor, R.J.M., 2016. Strategies towards statistically robust interpretations of in situ U-Pb zircon geochronology. Geosci. Front. 7, 581–589.

Stewart, J.H., Gehrels, G.E., Barth, A.P., Link, P.K., Christie-Blick, N., Wrucke, C.T., 2001. Detrital zircon provenance of Mesoproterozoic to Cambrian arenites in the western United States and northwestern Mexico. Geol. Soc. Am. Bull. 113, 1343–1356.

Sun, W.H., Zhou, M.F., Yan, D.P., Li, J.W., Ma, Y.X., 2008. Provenance and tectonic setting of the Neoproterozoic Yanbian Group, western Yangtze Block (SW China). Precambrian Res. 167, 213–236.

Sun, W.H., Zhou, M.F., Gao, J.F., Yang, Y.H., Zhao, X.F., Zhao, J.H., 2009. Detrital zircon U-Pb geochronological and Lu-Hf isotopic constraints on the Precambrian magmatic and crustal evolution of the western Yangtze Block, SW China. Precambrian Res. 172, 99–126.

Tapponnier, P., Xu, Z., Roger, F., Meyer, B., Arnaud, N., Wittlinger, G., Yang, J., 2001. Oblique stepwise rise and growth of the Tibet Plateau. Science 294, 1671–1677.

Tung, K.A., Yang, H.J., Yang, H.Y., Liu, D.Y., 2007a. SHRIMP U–Pb geochronology of the zircons from the Precambrian basement of the Qilian Block and its geological significances. Chin. Sci. Bull. 52, 2687–2701.

Tung, K.A., Yang, H.Y., Liu, D.Y., Zhang, J.X., Tseng, C.Y., Wan, Y.S., 2007b. SHRIMP U–Pb geochronology of the detrital zircons from the Longshoushan Group and its tectonic significance. Chin. Sci. Bull. 52, 1414–1425.

Tung, K.A., Yang, H.Y., Liu, D.Y., Zhang, J.X., Yang, H.J., Shau, Y.H., Tseng, C.Y., 2012. The amphibolite-facies metamorphosed mafic rocks from the Maxianshan area, Qilian block, NW China: a record of early Neoproterozoic arc magmatism. J. Asian Earth Sci. 46, 177–189.

Tung, K.A., Yang, H.Y., Liu, D.Y., Zhang, J.X., Yang, H.J., Sha, Y.H., 2013. The Neoproterozoic granitoids from the Qilian Block, NW China: evidence for a link between the Qilian and South China blocks. Precambrian Res. 235, 163–189.

Vermeesch, P., 2012. On the visualization of detrital age distributions. Chem. Geol. 312–313, 190–194.

Vermeesch, P., Resentini, A., Garzanti, E., 2016. An R package for statistical provenance analysis. Sediment. Geol. 336, 14–25.

Wan, Y.S., Liu, D.Y., Dong, C.Y., Yin, X.Y., 2011. SHRIMP zircon dating of metasedimentary rock from the Qinling Group in the north of Xixia, North Qinling Orogenic Belt: constraints on complex histories of source region and timing of deposition and metamorphism. Acta Petrol. Sin. 27, 1172–1178.

Wang, G.C., Wei, Q.R., Jia, C.X., Zhang, K.X., Li, D.W., Zhu, Y.H., Xiang, S.Y., 2007. Some ideas of Precambrian geology in the East Kunlun, China. Geol. Bull. China 26, 929–937 (in Chinese with English Abstract).

Wang, C., Zhao, X., Liu, Z., Lippert, P.C., Graham, S.A., Coe, R.S., Yi, H., Zhu, L., Liu, S., Li, Y., 2008. Constraints on the early uplift history of the Tibetan Plateau. Proc. Natl. Acad. Sci. 105, 4987–4992.

Wang, L.J., Griffin, W.L., Yu, J.H., O'Reilly, S.Y., 2010. Precambrian crustal evolution of the Yangtze Block tracked by detrital zircons from Neoproterozoic sedimentary rocks. Precambrian Res. 177, 131–144.

Wang, L.J., Yu, J.H., Griffin, W.L., O'Reilly, S.Y., 2012a. Early crustal evolution in the western Yangtze Block: evidence from U-Pb and Lu-Hf isotopes on detrital zircons from sedimentary rocks. Precambrian Res. 222, 368–385.

Wang, X., Hu, N., Wang, T., Sun, Y., Ju, S., Lu, X., Li, S., Qi, Q., 2012b. Late Ordovician Wanbaogou granitoid pluton from the southern margin of the Qaidam basin: Zircon SHRIMP U-Pb age, Hf isotope and geochemistry. Acta Petrol. Sin. 28, 2950–2962 (In Chinese with English Abstract).

Wang, L.J., Griffin, W.L., Yu, J.H., O'Reilly, S.Y., 2013. U-Pb and Lu-Hf isotopes in detrital zircon from Neoproterozoic sedimentary rocks in the northern Yangtze Block: implications for Precambrian crustal evolution. Gondwana Res. 23, 1261–1272.

Wang, C., Liu, L., Xiao, P.X., Cao, Y.T., Yu, H.Y., Meert, J.G., Liang, W.T., 2014. Geochemical and geochronologic constraints for Paleozoic magmatism related to the orogenic collapse in the North Qimantagh belth–South Altyn region, northwestern China. Lithos 202–203, 1–20.

Wang, G., Sun, F.Y., Li, B.L., Ao, C., Li, S.J., Zhao, J.W., Yang, Q.A., 2016b. Geochronology, geochemistry and tectonic implication of early Neoproterozoic monzogranite in Xiarihamu Ore District from East Kunlun. Geotecton. Metallog. 40, 1247–1260 (In Chinese with English Abstract).

Wang, Y., Li, Y., Wei, J., Li, H., Han, Y., Zhou, H., Huang, X., Ke, K., 2018. Origin of Late Silurian A-Type granite in Wulonggou Area, East Kunlun orogen: Zircon U-Pb age, geochemistry, Nd and Hf isotopic constraints. Earth Sci. 43, 1219–1236 (In Chinese with English Abstract).

Wei, Q., Li, D., Wang, G., 2007. Geochemical characteristics and tectonic setting of volcanic rocks from the Wanbaogou Group in East Kunlun orogenic belt. J. Mineral. Petrol. 27, 97–106 (In Chinese with English Abstract).

Wei, Y., Xiao, A., Wu, L., Mao, L., Zhao, H., Shen, Y., Wang, L., 2016. Temporal and spatial patterns of Cenozoic deformation across the Qaidam Basin, Northern Tibetan Plateau. Terra Nova 28, 409–418.

Weislogel, A.L., Graham, S.A., Chang, E.Z., Wooden, J.L., Gehrels, G.E., Yang, H., 2006. Detrital zircon provenance of the Late Triassic Songpan-Ganzi complex: sedimentary record of collision of the North and South China blocks. Geology 34, 97–100.

Weislogel, A.L., Graham, S.A., Chang, E.Z., Wooden, J.L., Gehrels, G.E., 2010. Detrital zircon provenance from three turbidite depocenters of the Middle-Upper Triassic Songpan–Ganzi complex, central China: record of collisional tectonics, erosional exhumation, and sediment production. Geol. Soc. Am. Bull. 122, 2041–2062.

Wu, C., Gao, Y., Wu, S., Chen, Q., 2007a. Zircon SHRIMP U-Pb dating of granites from the Da Qaidam area in the north margin of Qaidam basin, NW China. Acta Petrol. Sin. 23, 1861–1875 (In Chinese with English Abstract).

Wu, F.Y., Li, X.H., Zheng, Y.F., Gao, S., 2007b. Lu–Hf isotopic systematics and their applications in petrology. Acta Petrol. Sin. 23, 185–220 (In Chinese with English Abstract).

Wu, C., Gao, Y., Wu, S., Chen, Q., Wooden, J.L., Mazadab, F.K., Mattinson, C., 2008. Zircon SHRIMP dating and geochemical characteristics of granite from the Western Qaidam. Sci. China Earth Sci. 38, 930–949 (In Chinese).

Wu, L., Xiao, A., Wang, L., Shen, Z., Zhou, S., Chen, Y., Wang, L., Liu, D., Guan, J., 2011. Late Jurassic–Early Cretaceous northern Qaidam basin, NW China: implications for the earliest Cretaceous intracontinental tectonism. Cretac. Res. 32, 552–564.

Wu, C., Gao, Y., Lei, M., Qin, H., Liu, C., Li, M., Frost, B., Wooden, J., 2014a. Zircon SHRIMP U-Pb dating, Lu-Hf isotopic characteristics and petrogenesis of the Paleozoic granites in Mangya area, southern Altun, NW China. Acta Petrol. Sin. 30, 2297–2323 (In Chinese with English Abstract).

Wu, C., Gao, Y., Li, Z., Lei, M., Qin, H., Li, M., Liu, C., Frost, R.B., Robinson, P.T., Wooden, J.L., 2014b. Zircon SHRIMP U-Pb dating of granites from Dulan and the chronological framework of the North Qaidam UHP belt, NW China. Sci. China Earth Sci. 57, 2945–2965.

Wu, C., Yin, A., Zuza, A.V., Zhang, J., Liu, W., Ding, L., 2016. Pre-Cenozoic geologic history of the central and northern Tibetan Plateau and the role of Wilson cycles in constructing the Tethyan orogenic system. Lithosphere 8, 254–292.

Wu, C., Liu, C., Fan, S., Zuza, A.V., Ding, L., Liu, W., Zhou, Z., 2019a. Structural analysis and tectonic evolution of the western domain of the Eastern Kunlun Range, northwest Tibet. Geol. Soc. Am. Bull. https://doi.org/10.1130/B35388.1.

Wu, C., Zuza, A.V., Chen, X., Ding, L., Levy, D.A., Liu, C., Liu, W., Jiang, T., Stockli, D.F., 2019b. Tectonics of the Eastern Kunlun Range: Cenozoic reactivation of a Paleozoic-early Mesozoic orogen. Tectonics 38, 1609–1650.

Wu, C., Zuza, A.V., Zhou, Z., Yin, A., McRivette, M.W., Chen, X., Ding, L., Geng, J., 2019c. Mesozoic-Cenozoic evolution of the Eastern Kunlun Range, central Tibet, and implications for basin evolution during the Indo-Asian collision. Lithosphere 11, 524–550.

Wu, L., Lin, X., Cowgill, E., Xiao, A., Cheng, X., Chen, H., Zhao, H., Shen, Y., Yang, S., 2019d. Middle Miocene reorganization of the Altyn Tagh fault system, northern Tibetan Plateau. GSA Bull. 131, 1157–1178.

Xia, X.P., Sun, M., Zhao, G.C., Wu, F.Y., Xu, P., Zhang, J.H., Luo, Y., 2006a. U–Pb and Hf isotopic study of detrital zircons from the Wulashan khondalites: constraints on the evolution of the Ordos Terrane, Western Block of the North China Craton. Earth Planet. Sci. Lett. 241, 581–593.

Xia, X.P., Sun, M., Zhao, G.C., Luo, Y., 2006b. LA-ICP-MS U–Pb geochronology of detrital zircons from the Jining Complex, North China Craton and its tectonic significance. Precambrian Res. 144, 199–212.

Xiao, W.J., Windley, B.F., Chen, H.L., Zhang, G.C., Li, J.L., 2002. Carboniferous-Triassic subduction and accretion in the western Kunlun, China: implications for the collisional and accretionary tectonics of the northern Tibetan Plateau. Geology 30, 295–298.

Xiao, W.J., Windley, B.F., Liu, D.Y., Jian, P., Liu, C.Z., Yuan, C., Sun, M., 2005. Accretionary tectonics of the Western Kunlun Orogen, China: a Paleozoic–Early Mesozoic, long-lived active continental margin with implications for the growth of Southern Eurasia. J. Geol. 113, 687–705.

Xiao, W., Windley, B.F., Yong, Y., Yan, Z., Yuan, C., Liu, C., Li, J., 2009. Early Paleozoic to Devonian multiple-accretionary model for the Qilian Shan, NW China. J. Asian Earth Sci. 35, 323–333.

Xiong, F.-H., Ma, C.-Q., Zhang, J.-Y., Liu, B., 2012. The origin of mafic microgranular enclaves and their host granodiorites from East Kunlun, Northern Qinghai-Tibet Plateau: implications for magma mixing during subduction of Paleo-Tethyan lithosphere. Mineral. Petrol. 104, 211–224.

Xiong, F., Ma, C., Zhang, J., Liu, B., Jiang, H., 2014. Reworking of old continental lithosphere: an important crustal evolution mechanism in orogenic belts, as evidenced by Triassic I-type granitoids in the East Kunlun orogen, Northern Tibetan Plateau. J. Geol. Soc. 171, 847–863.

Xiong, F., Ma, C., Wu, L., Jiang, H.A., Liu, B., 2015. Geochemistry, zircon U-Pb ages and Sr-Nd-Hf isotopes of an Ordovician appinitic pluton in the East Kunlun orogen: new evidence for Proto-Tethyan subduction. J. Asian Earth Sci. 111, 681–697.

Xu, Z.Q., Yang, J.S., Zhang, J.X., Jiang, M., Li, H.B., Cui, J.W., 1999. A comparison between the tectonic units in two sides of the Altun sinistral strike-slip fault and the mechanism of lithospheric shearing. Acta Geol. Sin. 73, 193–205 (In Chinese with English Abstract).

Xu, W., Zhang, H., Liu, X., 2007. U-Pb zircon dating constraints on formation time of Qilian high-grade metamorphic rock and its tectonic implications. Chin. Sci. Bull. 52, 531–538.

Xu, Y.J., Cawood, P.A., Du, Y.S., Hu, L., Yu, W., Zhu, Y., Li, W., 2013a. Linking south China to northern Australia and India on the margin of Gondwana: constraints from detrital zircon U-Pb and Hf isotopes in Cambrian strata. Tectonics 32, 1547–1558.

Xu, Z.Q., He, B.Z., Zhang, C.L., Zhang, J.X., Wang, Z.M., Cai, Z.H., 2013b. Tectonic framework and crustal evolution of the Precambrian basement of the Tarim Block in NW China: new geochronological evidence from deep drilling samples. Precambrian Res. 235, 150–162.

Xu, X., Song, S., Su, L., 2016. Formation age and tectonic significance of the Wanbaogou basalts in the middle East Kunlun orogenic belt. Acta Petrol. Mineral. 35, 965–980 (In Chinese with English Abstract).

Yan, Z., Aitchison, J., Fu, C., Guo, X., Niu, M., Xia, W., Li, J., 2015. Hualong Complex, South Qilian terrane: U–Pb and Lu–Hf constraints on Neoproterozoic micro-continental fragments accreted to the northern Proto-Tethyan margin. Precambrian Res. 266, 65–85.

Yan, Q., Pei, X., Li, R., Li, Z., Pei, L., Liu, C., Chen, Y., Hu, C., Zhang, Y., Wang, X., Peng, S., 2017. Detrital zircon U-Pb age and geological significance of metamorphic strata at Gouli area in the Central tectonic belt of East Kunlun. Northwest. Geol. 50, 165–181 (In Chinese with English Abstract).

Yang, J.S., Robinson, P.T., Jiang, C.F., Xu, Z.Q., 1996. Ophiolites of the Kunlun Mountains, China and their tectonic implications. Tectonophysics 258, 215–231.

Yang, J.Z., Zeng, Q.D., Shen, Y.C., Li, G.M., Liu, T.B., 1999. Basic features and its tectonic significance of Yaziquan ophiolite belt in eatern Kunlun orogenic belt, Xinjiang. Geoscience 13, 309–314 (In Chinese with English Abstract).

Yang, J.S., Xu, Z.Q., Song, S.G., Zhang, J.X., Wu, C.L., Shi, R.D., Li, H.B., Brunel, M., Tapponnier, P., 2002a. Subduction of continental crust in the early palaeozoic North Qaidam ultrahigh-pressure metamorphic belt, NW China: evidence from the discovery of coesite in the belt. Acta Geograph. Sin.-English Edition 76, 63–68.

Yang, J.S., Xu, Z.Q., Zhang, J.X., Song, S.G., 2002b. Early Palaeozoic North Qaidam UHP metamorphic belt on the north-eastern Tibetan plateau and a paired subduction model. Terra Nova 14, 397–404.

Yang, C.H., Geng, Y.S., Du, L.L., Ren, L.D., Wang, X.S., Zhou, X.W., Yang, Z.S., 2009. The identification of the Grenvillian granite on the western margin of the Yangtze Block and its geological implications. Geol. China 36, 647–657 (In Chinese with English Abstract).

Yang, L., Song, S., Su, L., Allen, M.B., Niu, Y., Zhang, G., Zhang, Y., 2019. Heterogeneous oceanic arc volcanic rocks in the South Qilian accretionary belt (Qilian orogen, NW China). J. Petrol. 60, 85–116.

Yao, J., Shu, L., Santosh, M., 2011. Detrital zircon U-Pb geochronology, Hf-isotopes and geochemistry—new clues for the Precambrian crustal evolution of Cathaysia Block, South China. Gondwana Res. 20, 553–567.

Yao, W.H., Li, Z.X., Li, W.X., Li, X.H., Yang, J.H., 2014. From Rodinia to Gondwanaland: a tale of detrital zircon provenance analyses from the southern Nanhua Basin, South China. Am. J. Sci. 314, 278–313.

Yin, A., Harrison, T.M., 2000. Geologic evolution of the Himalayan-Tibetan orogen. Annu. Rev. Earth Planet. Sci. 28, 211–280.

Yin, A., Manning, C.E., Lovera, O., Menold, C.A., Chen, X., Gehrels, G.E., 2007. Early Paleozoic tectonic and thermomechanical evolution of ultrahigh-pressure (UHP) metamorphic rocks in the northern Tibetan Plateau, northwest China. Int. Geol. Rev. 49, 681–716.

Yu, J.H., O'Reilly, S.Y., Wang, L., Griffin, W.L., Zhang, M., Wang, R., Jiang, S., Shu, L., 2008. Where was South China in the Rodinia supercontinent? Evidence from U–Pb geochronology and Hf isotopes of detrital zircons. Precambrian Res. 164, 1–15.

Yu, S.Y., Zhang, J.X., del Real, P.G., Zhao, X.L., Hou, K.J., Gong, J.G., Li, Y.S., 2013. The Grenvillian orogeny in the Altun-Qilian-North Qaidam mountain belts of northern Tibet Plateau: constraints from geochemical and zircon U-Pb age and Hf isotopic study of magmatic rocks. J. Asian Earth Sci. 73, 372–395.

Yu, L., Xiao, A., Wu, L., Tian, Y., Rittner, M., Lou, Q., Pan, X., 2017. Provenance evolution of the Jurassic northern Qaidam Basin (West China) and its geological implications: evidence from detrital zircon geochronology. Int. J. Earth Sci. 106, 2713–2726.

Yu, S., Li, S., Zhang, J., Peng, Y., Somerville, I., Liu, Y., Wang, Z., Li, Z., Yao, Y., Li, Y., 2019a. Multistage anatexis during tectonic evolution from oceanic subduction to continental collision: a review of the North Qaidam UHP Belt, NW China. Earth Sci. Rev. 191, 190–211.

Yu, S., Li, S., Zhang, J., Liu, Y., Peng, Y., Sun, D., Li, Y., 2019b. Grenvillian orogeny in the Oulongbuluke Block, NW China: constraints from an ~1.1 Ga Andean-type arc magmatism and metamorphism. Precambrian Res. 320, 424–437.

Yu, S., Zhang, J., Li, S., Santosh, M., Li, Y., Liu, Y., Li, X., Peng, Y., Sun, D., Wang, Z., Lv, P., 2019c. TTG-adakitic-like (tonalitic-trondhjemitic) magmas resulting from partial melting of metagabbro under high-pressure condition during continental collision in the North Qaidam UHP terrane, Western China. Tectonics 38, 791–822.

Yue, Y., Ritts, B.D., Graham, S.A., Wooden, J.L., Gehrels, G.E., Zhang, Z., 2004. Slowing extrusion tectonics: lowered estimate of post-Early Miocene slip rate for the Altyn Tagh fault. Earth Planet. Sci. Lett. 217, 111–122.

Zhang, J.Y., Ma, C.Q., Xiong, F.H., Liu, B., 2012. Petrogenesis and tectonic significance of the Late Permian–Middle Triassic calc-alkaline granites in the Balong region, eastern Kunlun orogen, China. Geol. Mag. 149, 892–908.

Zhang, L.Y., Ding, L., Pullen, A., Xu, Q., Liu, D.L., Cai, F.L., Yue, Y.H., Lai, Q.Z., Shi, R.D., Ducea, M.N., Kapp, P., Chapman, A., 2014. Age and geochemistry of western Hoh-Xil-Songpan-Ganzi granitoids, northern Tibet: Implications for the Mesozoic closure of the Paleo-Tethys ocean. Lithos 190–191, 328–348.

Zhang, F.F., Wang, X.L., Wang, D., Yu, J.H., Zhou, X.H., Sun, Z.M., 2017a. Neoproterozoic backarc basin on the southeastern margin of the Yangtze block during Rodinia assembly: new evidence from provenance of detrital zircons and geochemistry of mafic rocks. Geol. Soc. Am. Bull. 129, 904–919.

Zhang, J., Yu, S., Mattinson, C.G., 2017b. Early Paleozoic polyphase metamorphism in northern Tibet, China. Gondwana Res. 41, 267–289.

Zhang, Y., Song, S., Yang, L., Su, L., Niu, Y., Allen, M.B., Xu, X., 2017c. Basalts and picrites from a plume-type ophiolite in the South Qilian Accretionary Belt, Qilian Orogen: accretion of a Cambrian Oceanic Plateau? Lithos 278, 97–110.

Zhang, Q., Ding, Q., Song, K., Cheng, L., 2018a. Detrital zircon U-Pb geochronology and Hf isotope of phyllite of Langyashan Formation in Hongshuihe iron ore district of Eastern Kunlun and their geological significance. J. Jilin Univ. (Earth Sci. Ed.) 48, 1085–1104 (In Chinese with English Abstract).

Zhang, W., Jian, X., Fu, L., Feng, F., Guan, P., 2018b. Reservoir characterization and hydrocarbon accumulation in late Cenozoic lacustrine mixed carbonate-siliciclastic fine-grained deposits of the northwestern Qaidam basin, NW China. Mar. Pet. Geol. 98, 675–686.

Zhao, G., Wang, Y., Huang, B., Dong, Y., Li, S., Zhang, G., Yu, S., 2018. Geological reconstructions of the East Asian blocks: From the breakup of Rodinia to the assembly of Pangea. Earth Sci. Rev. 186, 262–286.

Zheng, Z., Chen, Y.J., Deng, X.H., Yue, S.W., Chen, H.J., Wang, Q.F., 2018. Origin of the Bashierxi monzogranite, Qiman Tagh, East Kunlun Orogen, NW China: a magmatic response to the evolution of the Proto-Tethys Ocean. Lithos 296, 181–194.

Zhou, M.F., Yan, D.P., Kennedy, A.K., Li, Y., Ding, J., 2002. SHRIMP U–Pb zircon geochronological and geochemical evidence for Neoproterozoic arc-magmatism along the western margin of the Yangtze Block, South China. Earth Planet. Sci. Lett. 196, 51–67.

Zhou, M.F., Ma, Y., Yan, D.P., Xia, X., Zhao, J.H., Sun, M., 2006. The Yanbian terrane (Southern Sichuan Province, SW China): a Neoproterozoic arc assemblage in the western margin of the Yangtze block. Precambrian Res. 144, 19–38.

Zhou, B., Dong, Y., Zhang, F., Yang, Z., Sun, S., He, D., 2016. Geochemistry and zircon U-Pb geochronology of granitoids in the East Kunlun Orogenic Belt, northern Tibetan Plateau: origin and tectonic implications. J. Asian Earth Sci. 130, 265–281.

Zhu, Y., Lin, Q., Jia, C., Wang, G., 2006. SHRIMP zircon U-Pb age and significance of Early Paleozoic volcanic rocks in East Kunlun orogenic belt, Qinghai Province, China. Science in China Series D 49, 88–96.

Zhu, W., Zheng, B., Shu, L., Ma, D., Wu, H., Li, Y., Huang, W., Yu, J., 2011a. Neoproterozoic tectonic evolution of the Precambrian Aksu blueschist terrane, northwestern Tarim, China: insights from LA-ICP-MS zircon U–Pb ages and geochemical data. Precambrian Res. 185, 215–230.

Zhu, X.Y., Chen, F.K., Li, S.Q., Yang, Y.Z., Nie, H., Siebel, W., Zhai, M.G., 2011b. Crustal evolution of the North Qinling terrain of the Qinling Orogen, China: evidence from detrital zircon U–Pb ages and Hf isotopic composition. Gondwana Res. 20, 194–204.

Zhuang, G., Hourigan, J.K., Ritts, B.D., Kent-Corson, M.L., 2011. Cenozoic multiple-phase tectonic evolution of the northern Tibetan plateau: constraints from sedimentary records from Qaidam basin, Hexi corridor, and Subei basin, northwest China. Am. J. Sci. 311, 116–152.

Zuza, A.V., Wu, C., Reith, R.C., Yin, A., Li, J., Zhang, J., Zhang, Y., Wu, L., Liu, W., 2018. Tectonic evolution of the Qilian Shan: an early Paleozoic orogen reactivated in the Cenozoic. GSA Bull. 130, 881–925.